CMB polarization as a probe of the early and late Universe

Josquin ERRARD

Orsay — Oct 12, 2017

CMB polarization as a probe of ~~the early and late Universe~~ dark energy properties and modified gravity

Josquin ERRARD

Orsay — Oct 12, 2017

Outline

- CMB lensing and evidence for DE
- Latest cosmological constraints from Planck
- Upcoming CMB observations and expected performance

POLARBEAR telescope
5,200m, Atacama desert, Chile

Cosmic Microwave Background (CMB)

zooming at the 10^{-5} level

Cosmic Microwave Background (CMB)

zooming at the 10^{-5} level

why are fluctuations so small?
… and why are there fluctuations?

Cosmic Microwave Background (CMB)

zooming at the 10^{-5} level

why are fluctuations so small?
… and why are there fluctuations?

Cosmic Microwave Background (CMB)

Observations are in remarkable agreement with single-field slow-roll inflation:

- **Super-horizon fluctuation**
- **Adiabaticity**
- **Gaussianity**
- **$n_s < 1$**

[see talk tomorrow by Martin Kuntz, Sophie Henrot-Versille]

zooming at the 10^{-7} level

zooming at the 10^{-7} level

➤ but we want gravitational waves in addition!

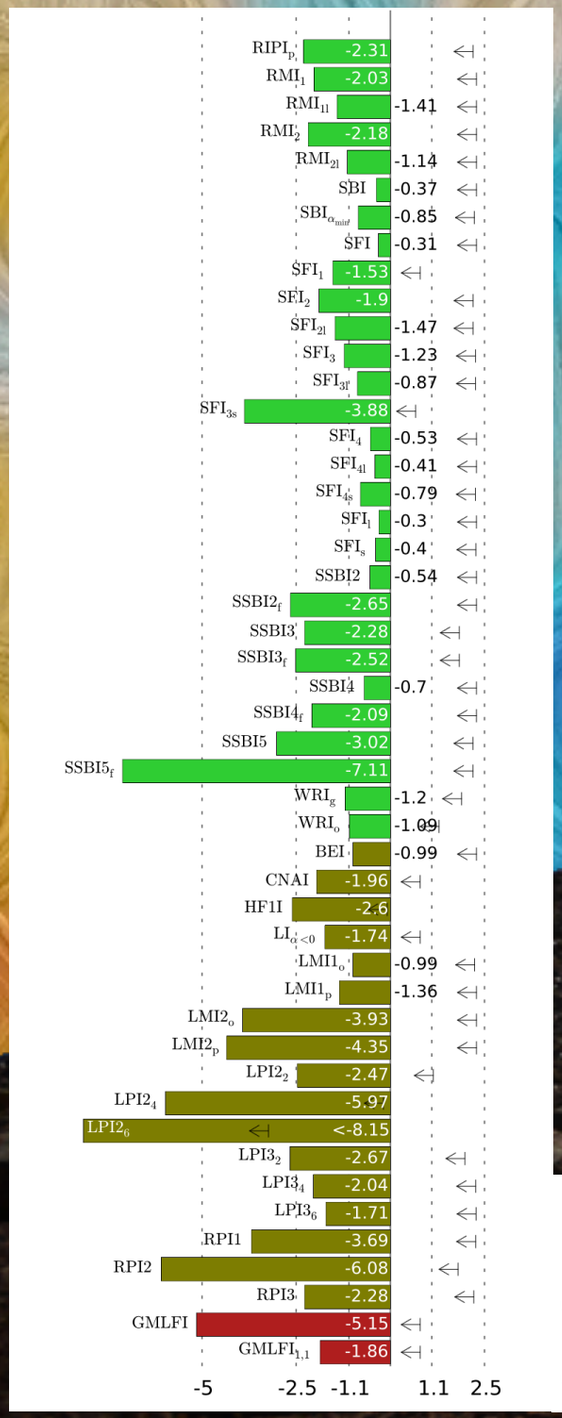

Parameter	Meaning	Physical Origin	Current Status
A_s	Scalar amplitude	H, $\dot{H}$, c_s	$(2.13 \pm 0.05) \times 10^{-9}$
n_s	Scalar tilt	$\dot{H}$, $\ddot{H}$, $\dot{c}_s$	0.965 ± 0.005
$dn_s/d\ln k$	Scalar running	$\dddot{H}$, $\ddot{c}_s$	only upper limits
A_t	Tensor amplitude	H	only upper limits
n_t	Tensor tilt	$\dot{H}$	only upper limits
r	Tensor-to-scalar ratio	$\dot{H}$, c_s	only upper limits
Ω_k	Curvature	Initial conditions	only upper limits
f_{NL}	Non-Gaussianity	Extra fields, sound speed, $\cdots$	only upper limits
S	Isocurvature	Extra fields	only upper limits
$G\mu$	Topological defects	End of inflation	only upper limits

Table 1: Summary of key parameters in inflationary cosmology, together with their likely physical origins and current observational constraints. At present, only upper limits exist for all parameters except A_s and n_s [5].

Exploring Cosmic Origins with CORE: Inflation
F. Finelli, M. Bucher et al., JCAP, 2017

The Best Inflationary Models After Planck
J. Martin, C. Ringeval, R. Trotta, V. Vennin, JCAP, 2014

gravitational lensing = remapping of the CMB fields

gravitational lensing = remapping of the CMB fields

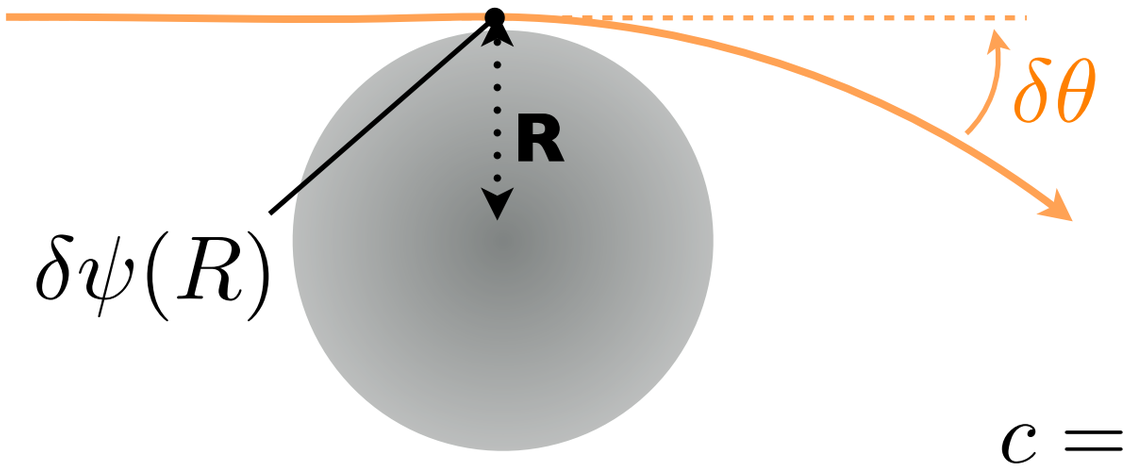

$$\delta\theta \simeq \frac{2\delta\psi(R)}{c^2}$$

Weak Gravitational Lensing of the CMB, A. Lewis & S. Challinor (2008)

$$c = 1 \qquad \delta\psi \simeq 2 \times 10^{-5} \longrightarrow \delta\theta \simeq 10^{-4}$$

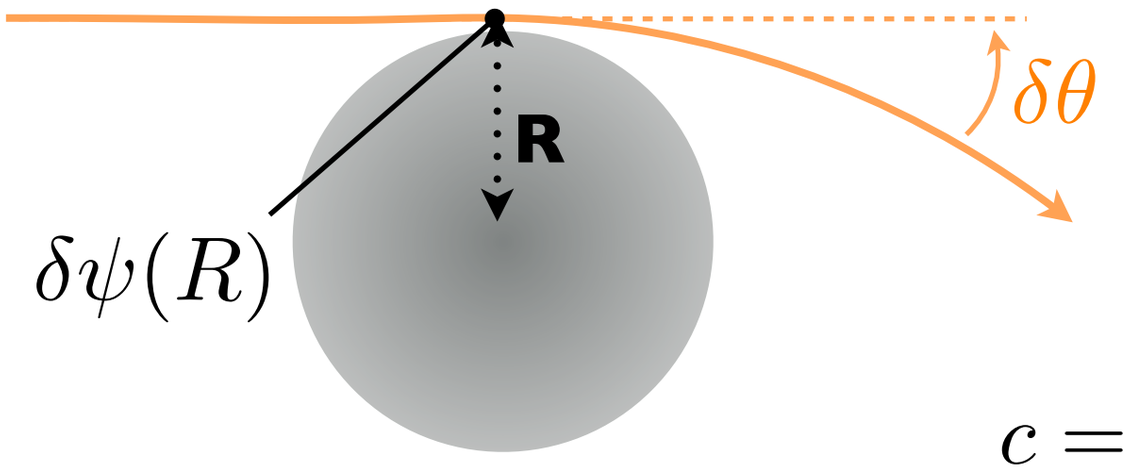

$$\delta\theta \simeq \frac{2\delta\psi(R)}{c^2}$$

Weak Gravitational Lensing of the CMB, A. Lewis & S. Challinor (2008)

$$c = 1 \qquad \delta\psi \simeq 2 \times 10^{-5} \longrightarrow \delta\theta \simeq 10^{-4}$$

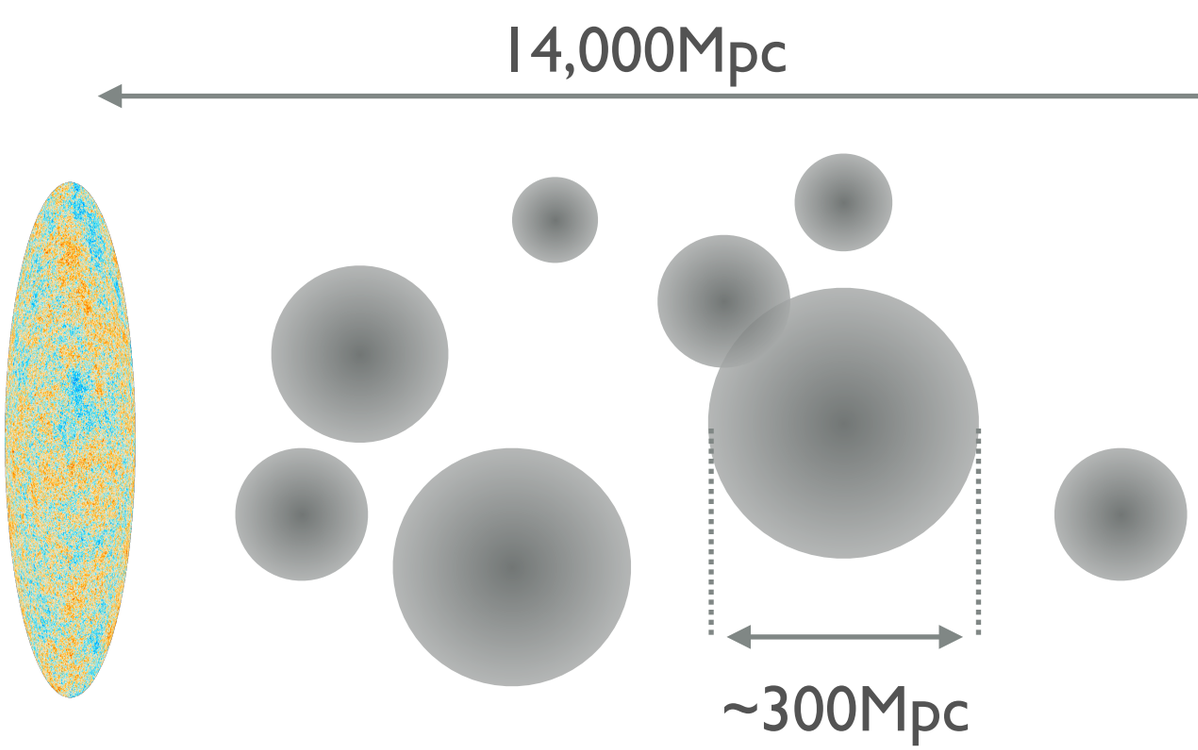

CMB photon encounters ~ 50 potential wells

$rms. \sim \sqrt{50} \times 10^{-4} \simeq 7 \times 10^{-4} \rightarrow \sim 2\mathrm{arcmin}$

$\frac{300}{7000} \sim 2\,\mathrm{deg}$ correlation scale due to a well mid-way to CMB last scattering surface. This means that lensing can have an important effect on the scale of the primary acoustic peaks.

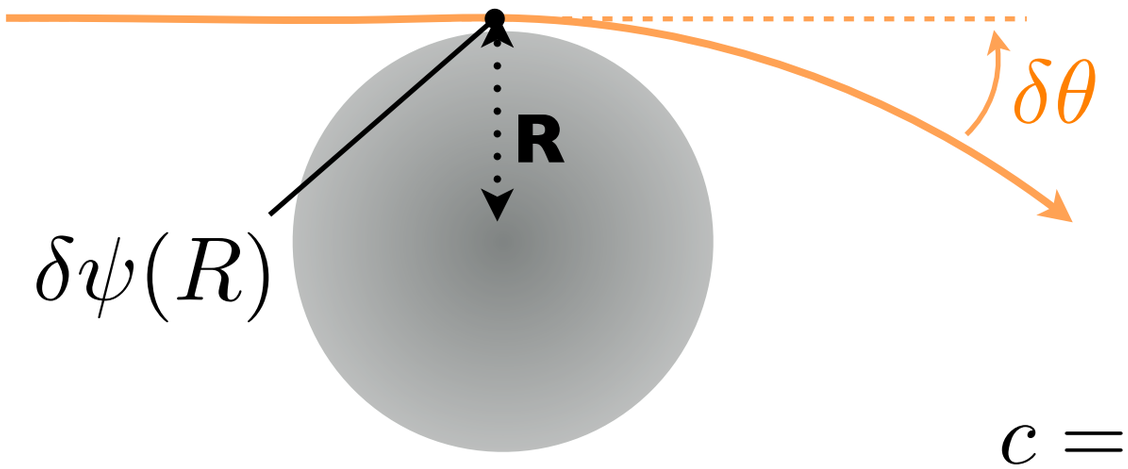

$$\delta\theta \simeq \frac{2\delta\psi(R)}{c^2}$$

Weak Gravitational Lensing of the CMB, A. Lewis & S. Challinor (2008)

$$c = 1 \qquad \delta\psi \simeq 2 \times 10^{-5} \longrightarrow \delta\theta \simeq 10^{-4}$$

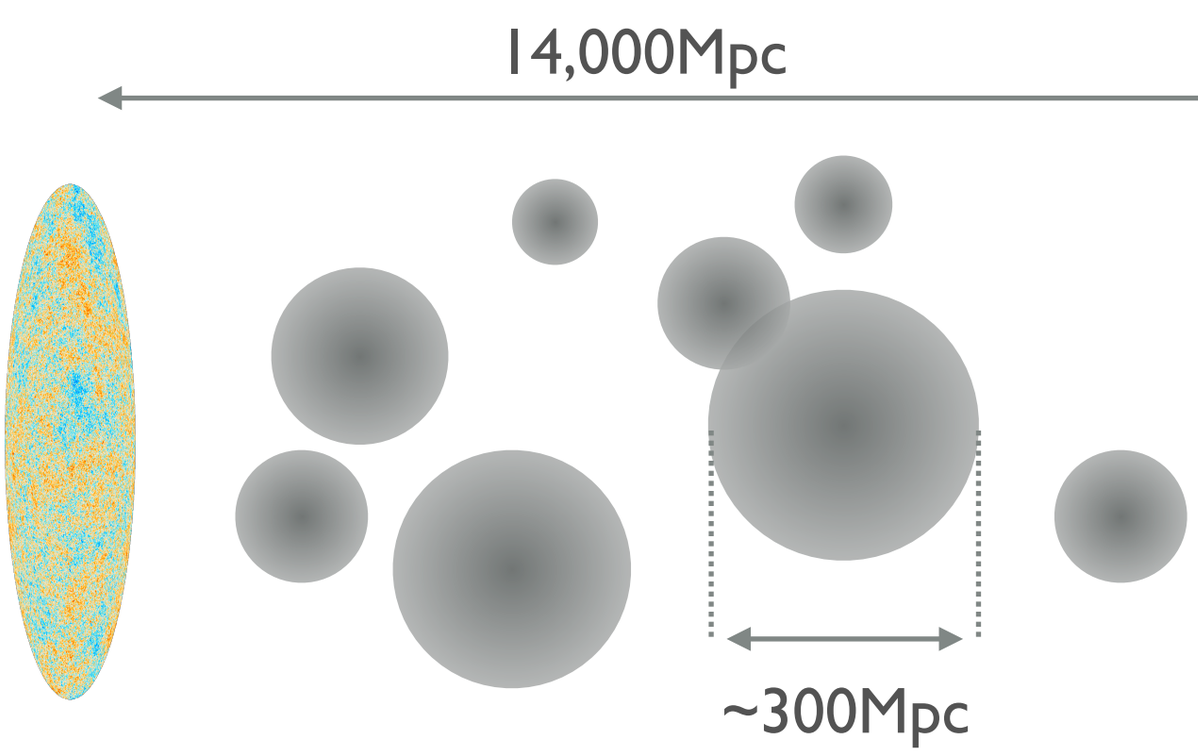

CMB photon encounters ~ 50 potential wells

$rms. \sim \sqrt{50} \times 10^{-4} \simeq 7 \times 10^{-4} \rightarrow \sim 2\mathrm{arcmin}$

$\frac{300}{7000} \sim 2\,\mathrm{deg}$ correlation scale due to a well mid-way to CMB last scattering surface. This means that lensing can have an important effect on the scale of the primary acoustic peaks.

Averaged over the sky, lensing smoothes out the power spectrum

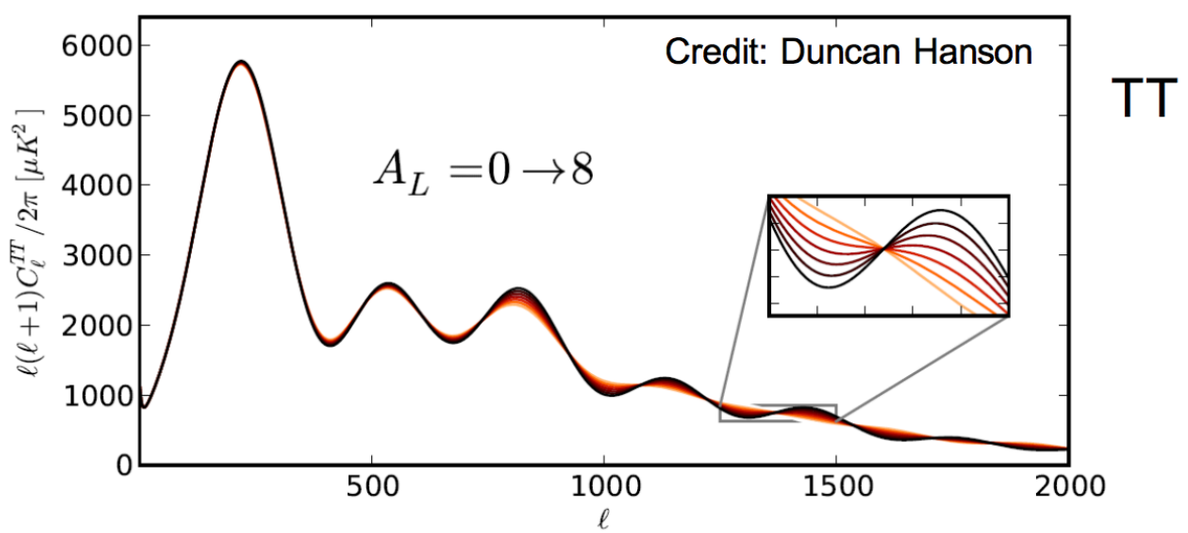

TT

primordial CMB

credits: Dominic Beck

observed CMB

credits: Dominic Beck

observed CMB

$\vec{\alpha} = \vec{\nabla}\psi$

credits: Dominic Beck

deflection field angular power spectrum

last scattering surface

growth factor or matter perturbation since decoupling

$$\frac{\ell^2}{4} C_\ell^{dd} = \int_0^{\eta_*} d\eta W^2(\eta) \left[\frac{D(\eta)}{a(\eta)}\right]^2$$

conformal time

scale factor

growth

geometry + projection term

comoving angular diameter distance

$$W(\eta) = \frac{3}{2}\Omega_m H_0^2 \frac{d_A(\eta_* - \eta)}{d_A(\eta_*)} P^{-1/2}\left(k = \frac{\ell + 1/2}{d_A(\eta)}, \eta_*\right)$$

Hubble constant

matter power spectrum at decoupling

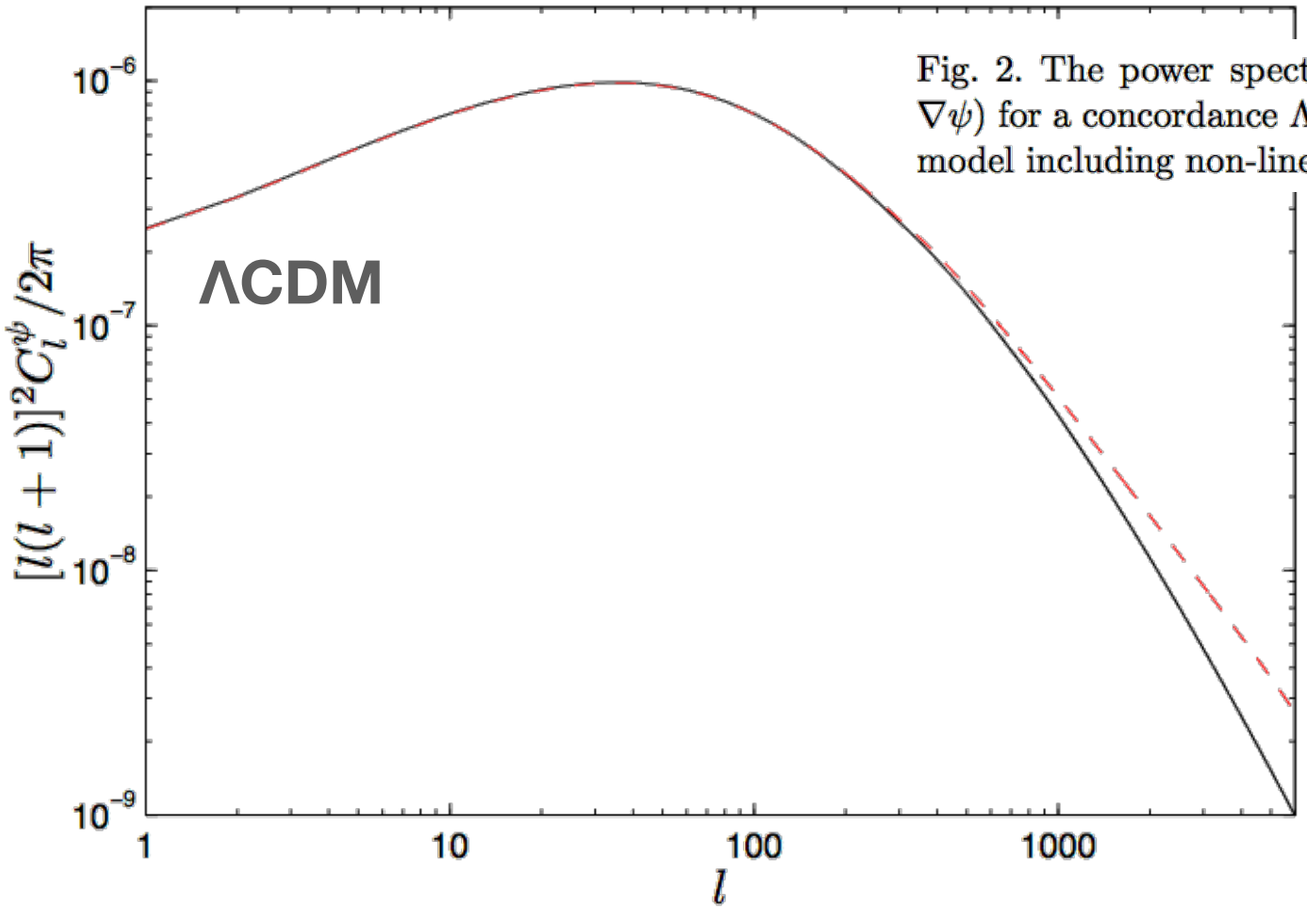

Fig. 2. The power spectrum of the deflection angle (given in terms of the lensing potential ψ by $\nabla\psi$) for a concordance ΛCDM model. The linear theory spectrum (solid) is compared with the same model including non-linear corrections (dashed) from HALOFIT (65).

Weak Gravitational Lensing of the CMB, A. Lewis & S. Challinor (2008)

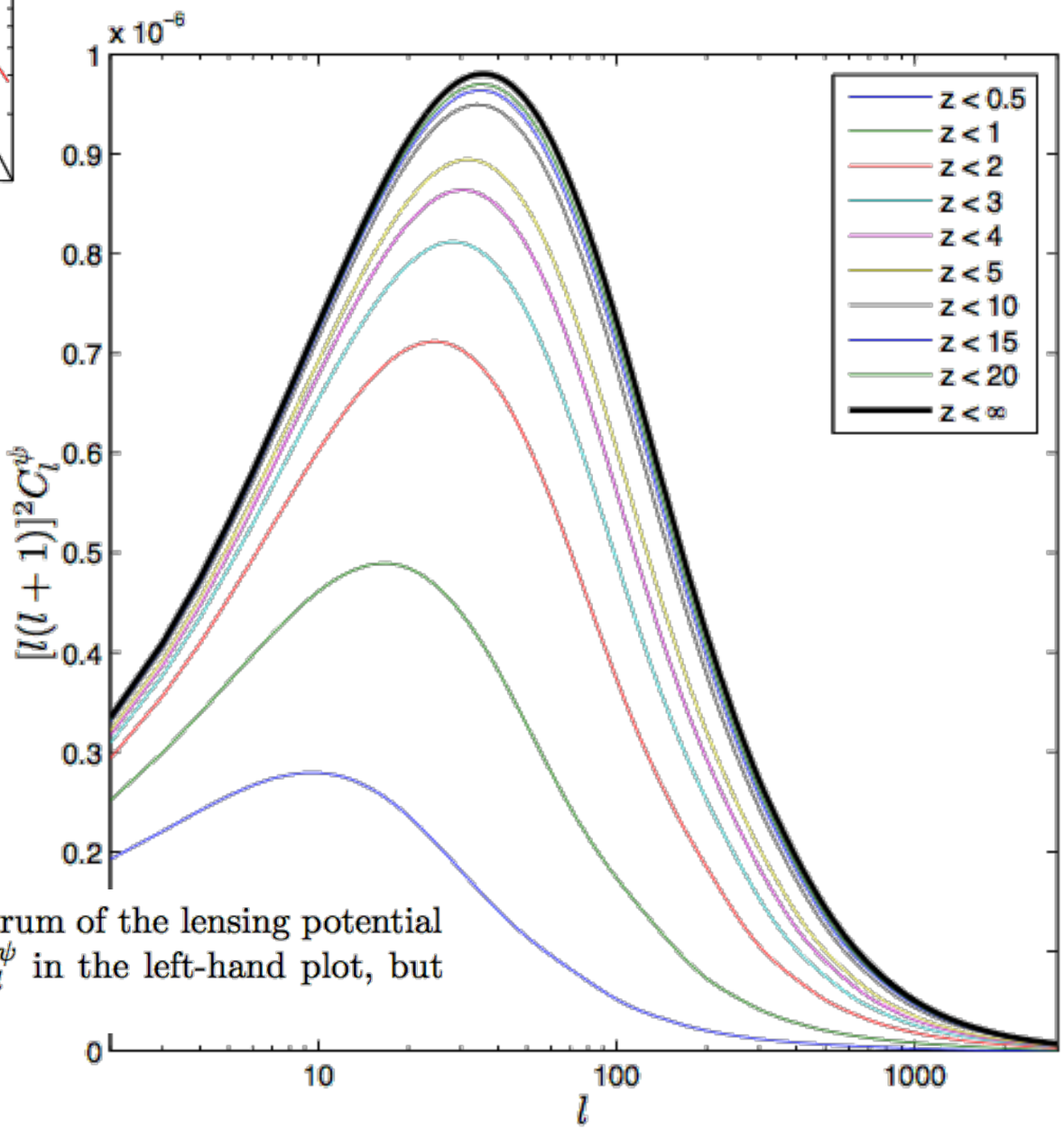

Fig. 3. Cumulative contribution of different redshifts to the power spectrum of the lensing potential for a concordance ΛCDM model. Note we have used a log scale for C_l^ψ in the left-hand plot, but linear in the right-hand plot.

(1) Quadratic estimators

↳ measure off-diagonal covariance induced by lensing (Hu+Okamoto 2001)

$$\tilde{\psi}(\mathbf{L}) \equiv N(\mathbf{L}) \int \frac{d^2\mathbf{l}}{2\pi} X^{\rm obs}(\mathbf{l}) X^{\rm obs\,*}(\mathbf{l}-\mathbf{L}) g(\mathbf{l},\mathbf{L})$$

- fast to implement
- nearly optimal for current (stage-II, -III) observations

(2) Maximum likelihood

$$-2\log(\mathcal{L}\left(X^{\rm obs}|\alpha\right)) = X^T\left(\mathbf{C}_\alpha\right)^{-1} X + \log\det\left(\mathbf{C}_\alpha\right)$$

- more expensive, but tractable iteratively (Hirata+Seljak 2003, Carron+Lewis 2017)
- better reconstruction for CMB-S4-like noise levels

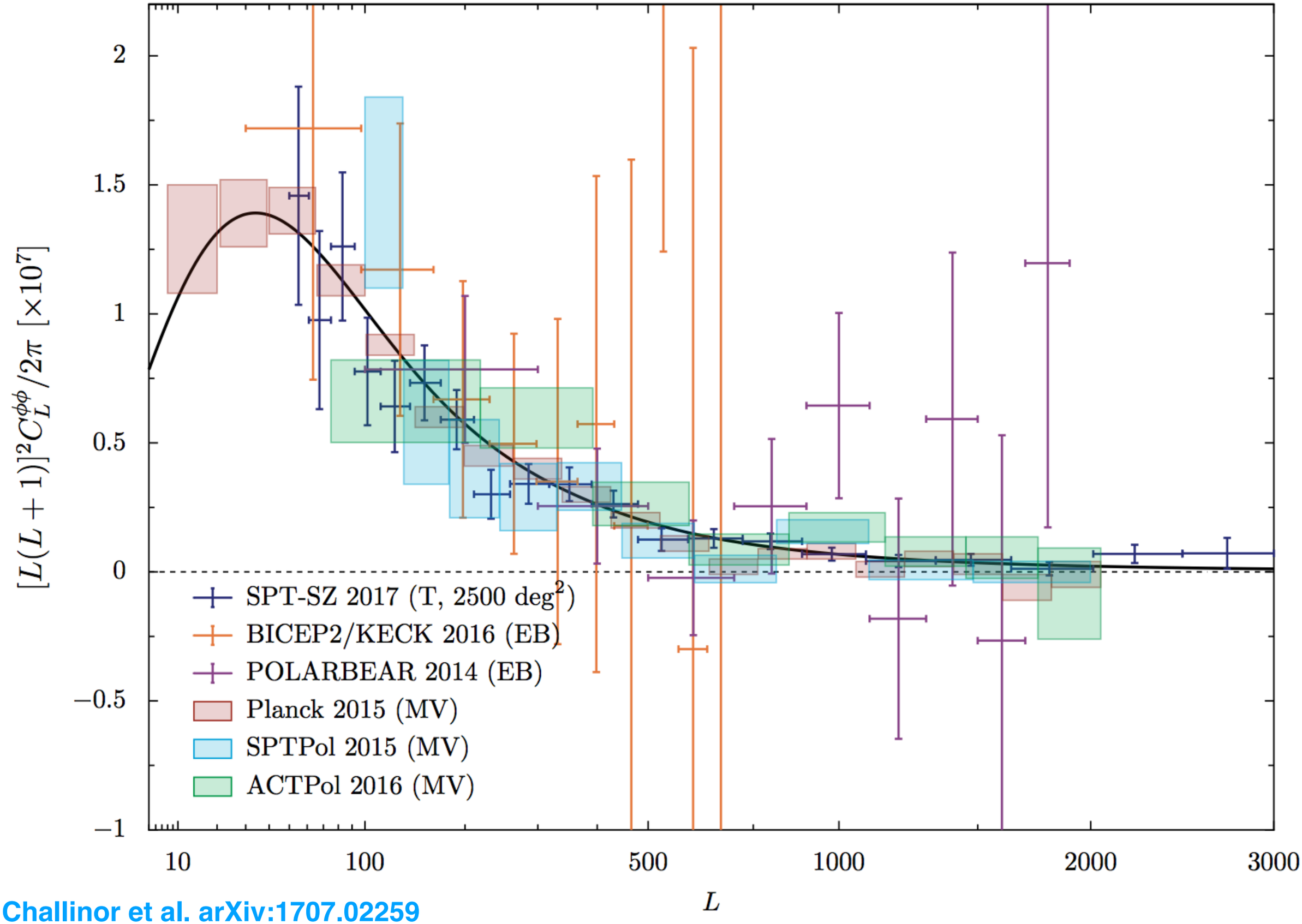

Challinor et al. arXiv:1707.02259

Evidence for dark energy from the cosmic microwave background alone using the Atacama Cosmology Telescope lensing measurements, Sherwin et al. (2011) arXiv:1105.0419

- **the spatially flat ΛCDM model with dark energy which best fits the WMAP seven-year data**
- **a model with positive spatial curvature but without dark energy.**

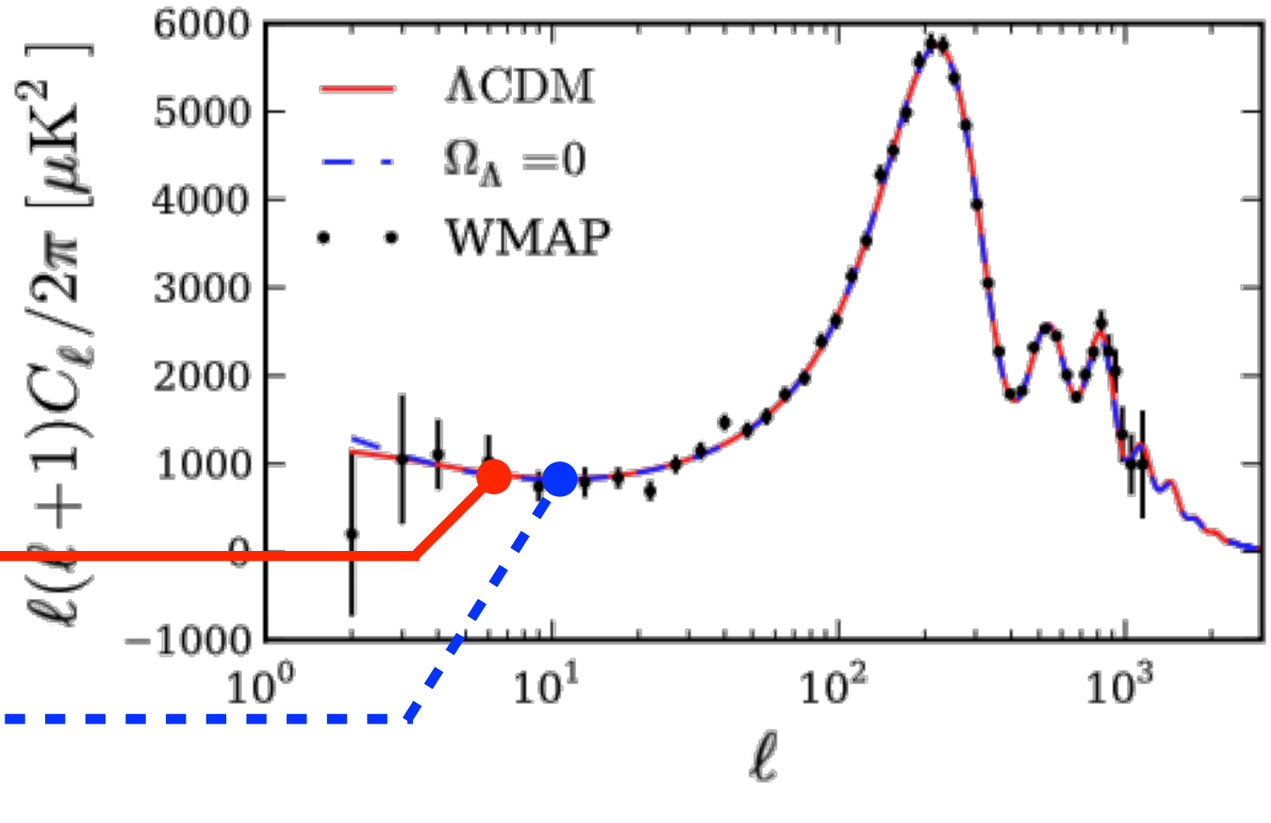

Evidence for dark energy from the cosmic microwave background alone using the Atacama Cosmology Telescope lensing measurements, Sherwin et al. (2011) arXiv:1105.0419

- **the spatially flat ΛCDM model with dark energy which best fits the WMAP seven-year data**
- **a model with positive spatial curvature but without dark energy.**

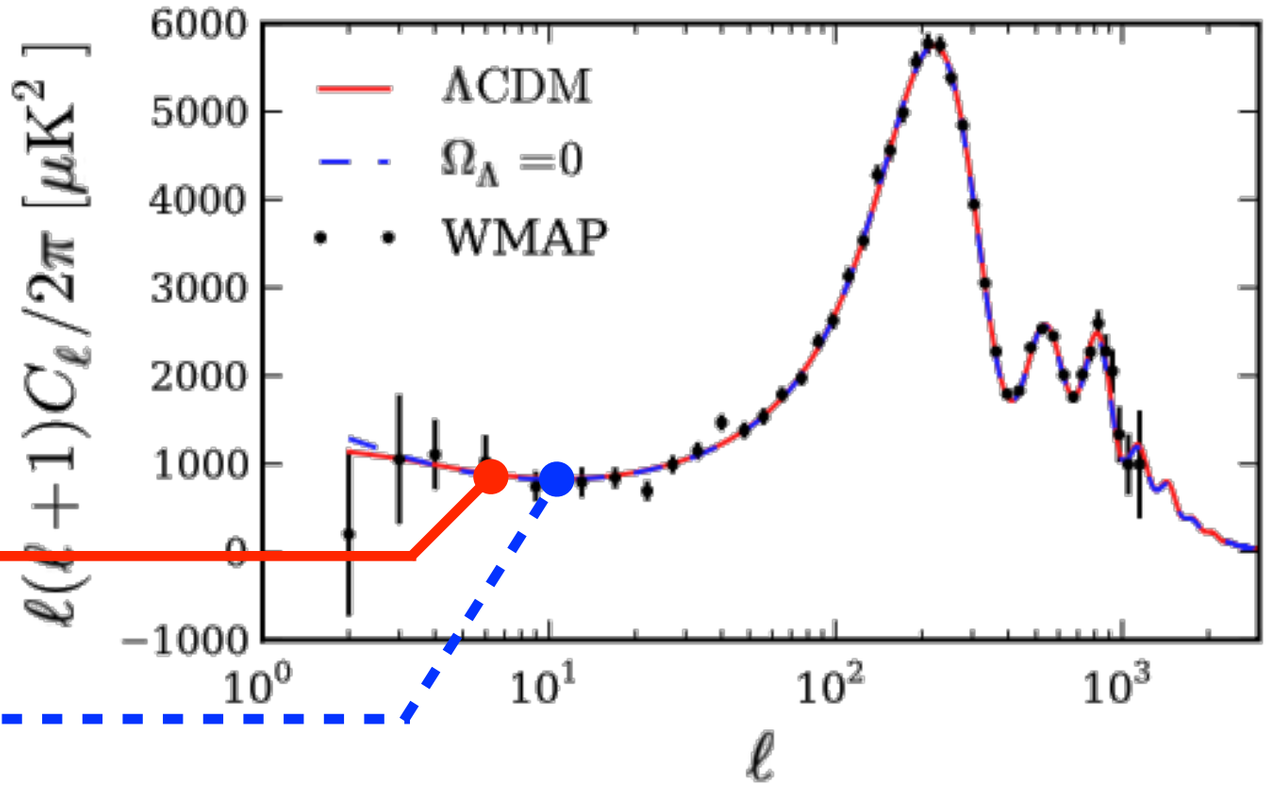

"These two cosmologies predict **significantly different CMB lensing deflection** power spectra C^{dd}.

Fig. on the right shows that the universe with $\Omega_\Lambda = 0$ produces more lensing on all scales. The **ACT measurements are a better fit to the model with vacuum energy** than to the model without dark energy."

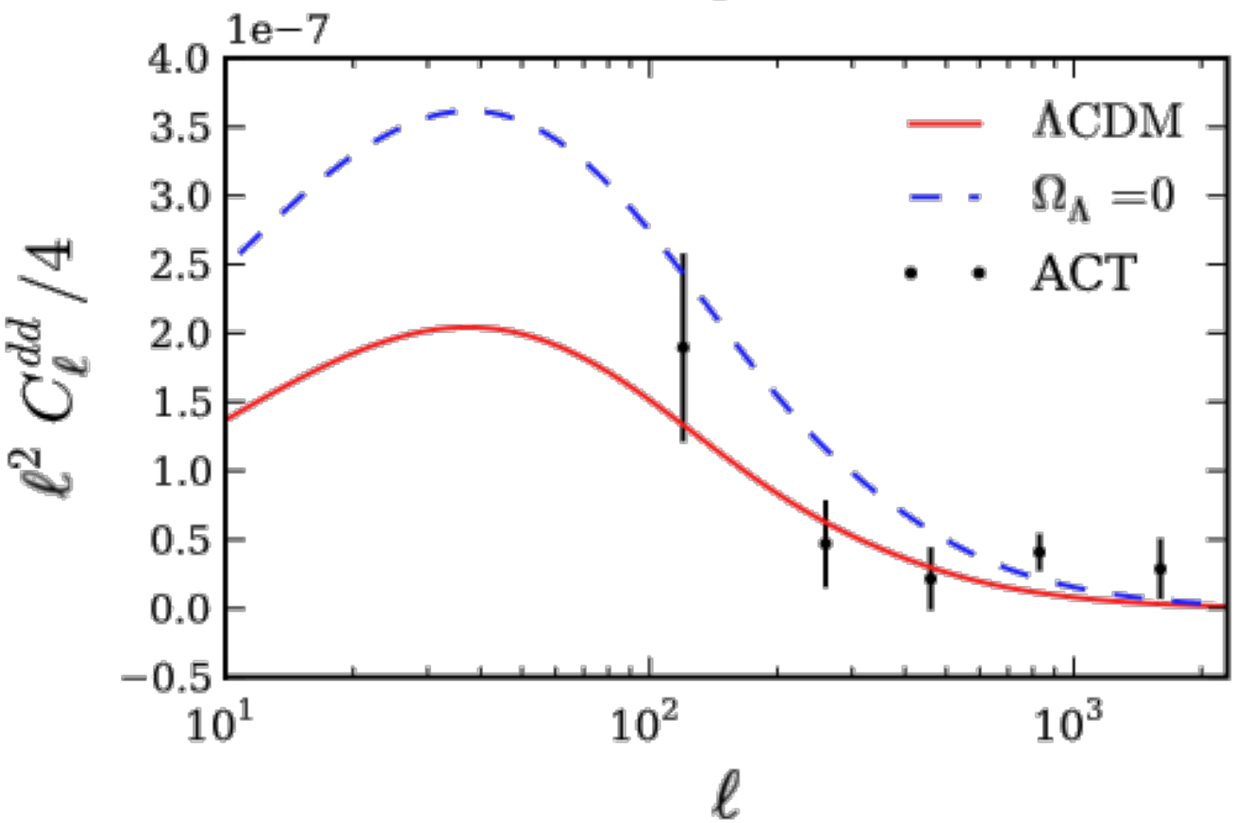

Planck 2015 results. XIV. Dark energy and modified gravity (2015)

$$w = w_0 + (1 - a)w_a$$

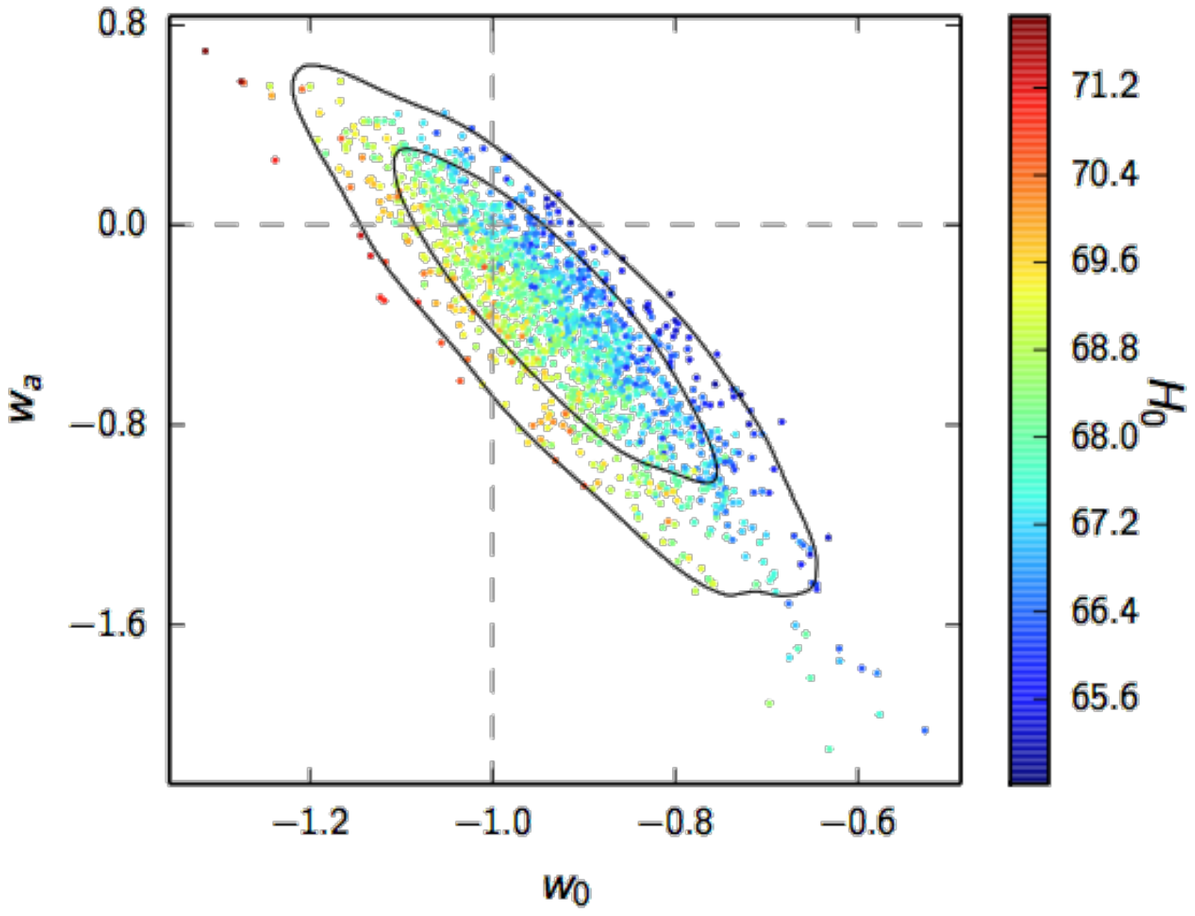

Fig. 27. Samples from the distribution of the dark energy parameters w_0 and w_a using *Planck* TT+lowP+BAO+JLA data, colour-coded by the value of the Hubble parameter H_0. Contours show the corresponding 68 % and 95 % limits. Dashed grey lines intersect at the point in parameter space corresponding to a cosmological constant.

$$w = -1.023^{+0.091}_{-0.096} \quad \textit{Planck}\ \text{TT+lowP+ext}; \tag{52a}$$

$$w = -1.006^{+0.085}_{-0.091} \quad \textit{Planck}\ \text{TT+lowP+lensing+ext}; \tag{52b}$$

$$w = -1.019^{+0.075}_{-0.080} \quad \textit{Planck}\ \text{TT, TE, EE+lowP+lensing+ext}.$$

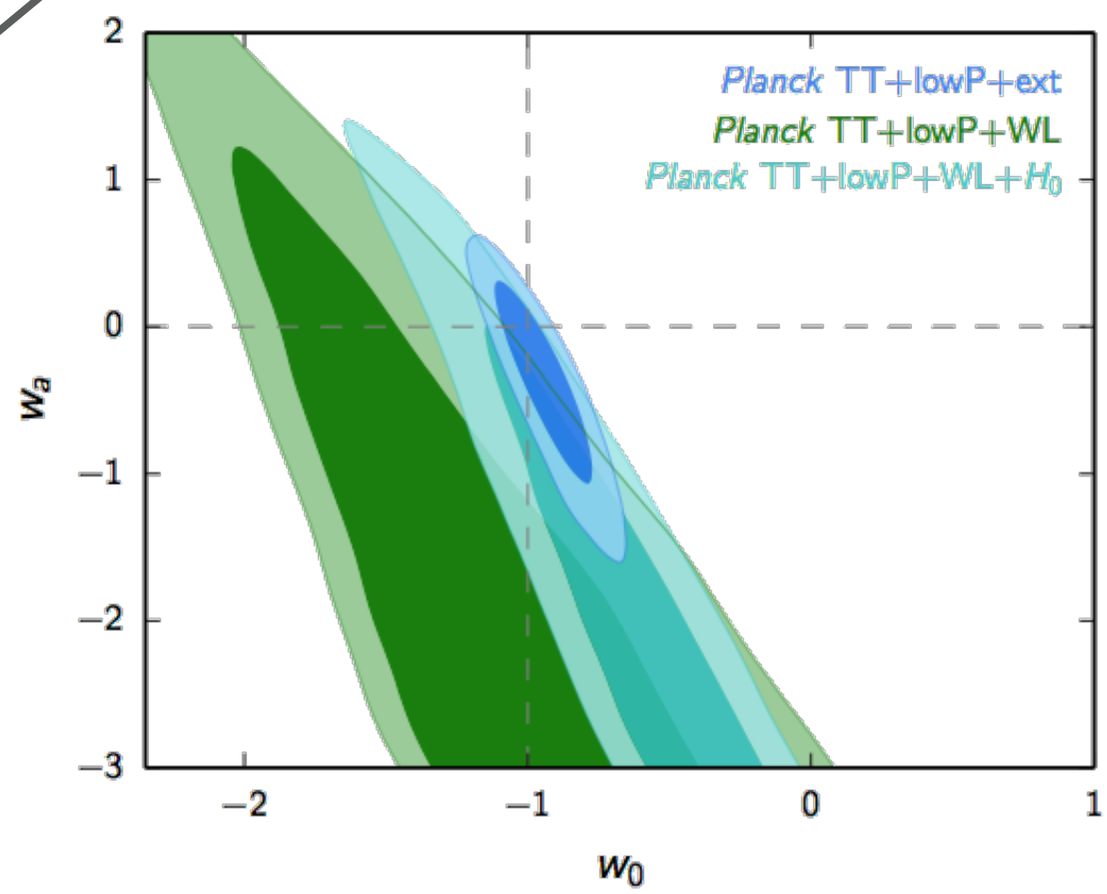

Fig. 28. Marginalized posterior distributions for (w_0, w_a) for various data combinations. We show *Planck* TT+lowP in combination with BAO, JLA, H_0 ("ext"), and two data combinations which add the CFHTLenS data with ultra-conservative cuts as described in the text (denoted "WL"). Dashed grey lines show the parameter values corresponding to a cosmological constant.

Planck 2015 results. XIV. Dark energy and modified gravity (2015)

Simple quintessence model

$$w(a) = w_0 + \sum_{i=1}^{N} (1-a)^i w_i \,.$$

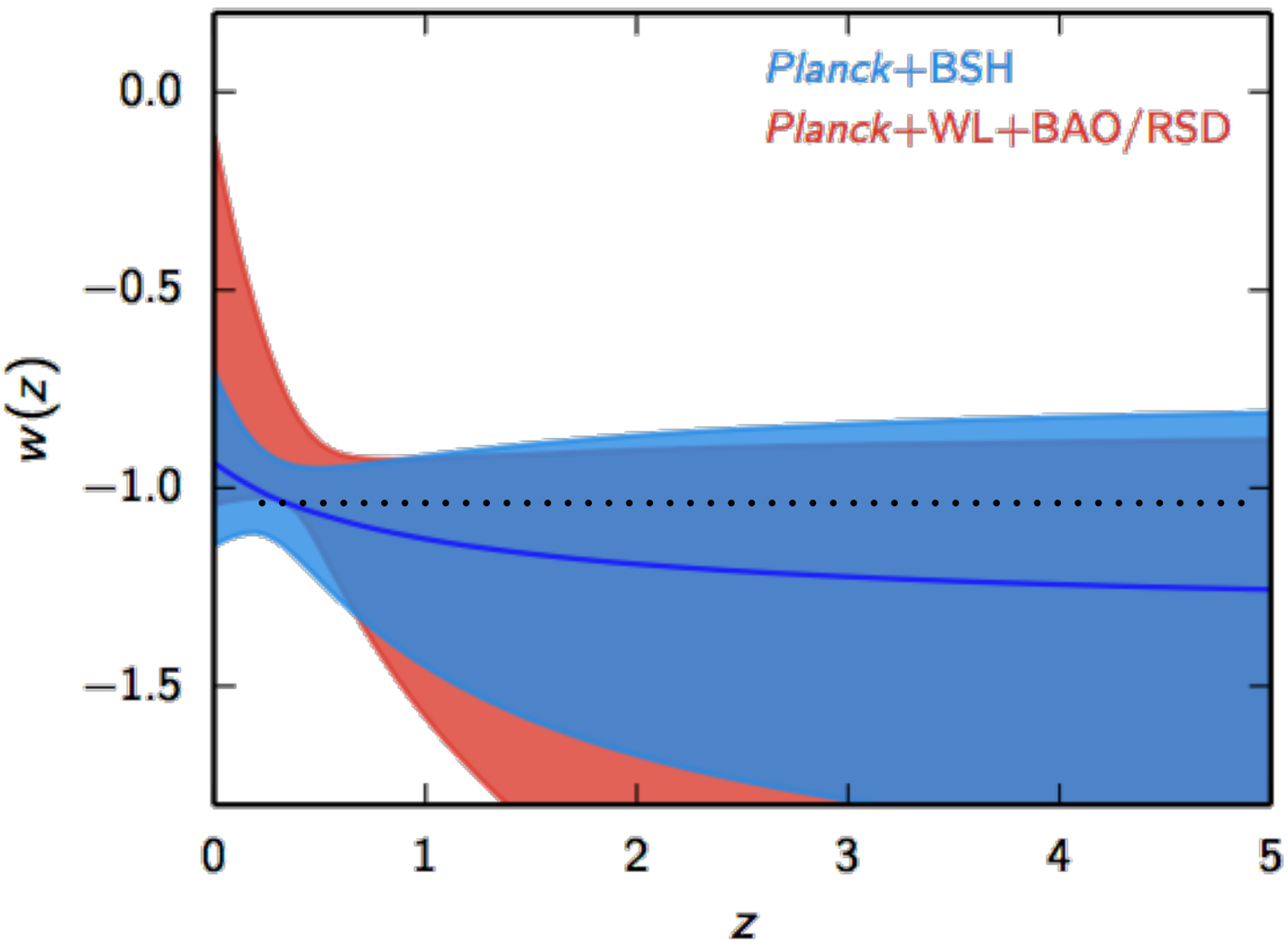

Fig. 5. Reconstructed equation of state $w(z)$ as a function of redshift (see Sect. 5.1.1), when assuming a Taylor expansion of $w(z)$ to first-order ($N = 1$ in Eq. 19), for different combinations of the data sets. The coloured areas show the regions which contain 95 % of the models. The central blue line is the median line for *Planck* TT+lowP+BSH. Here *Planck* indicates *Planck* TT+lowP.

Planck 2015 results. XIV. Dark energy and modified gravity (2015)

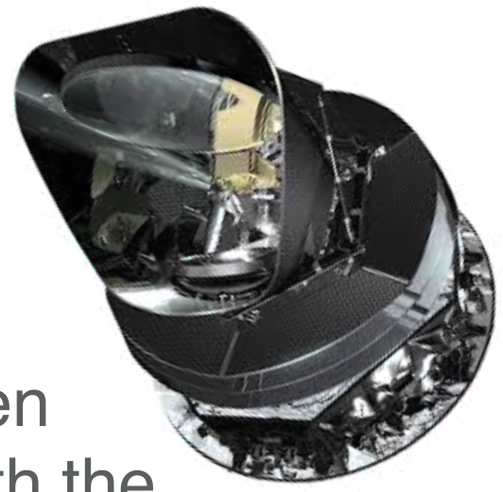

"The quest for Dark Energy and Modified Gravity is far from over. A **variety of different theoretical scenarios** have been proposed in literature and need to be carefully compared with the data. This effort is still in its early stages, given the variety of theories and parameterizations that have been suggested, together with a **lack of well tested numerical codes** that allow us to make detailed predictions for the desired range of parameters."

[see talks by Martin Kuntz and David Langlois]

➤ independently of the chosen parametrization for DE, data sets are compatible with ΛCDM

How is the CMB moving forward?

CMB-S4 Science Book, arXiv: 1610.02743

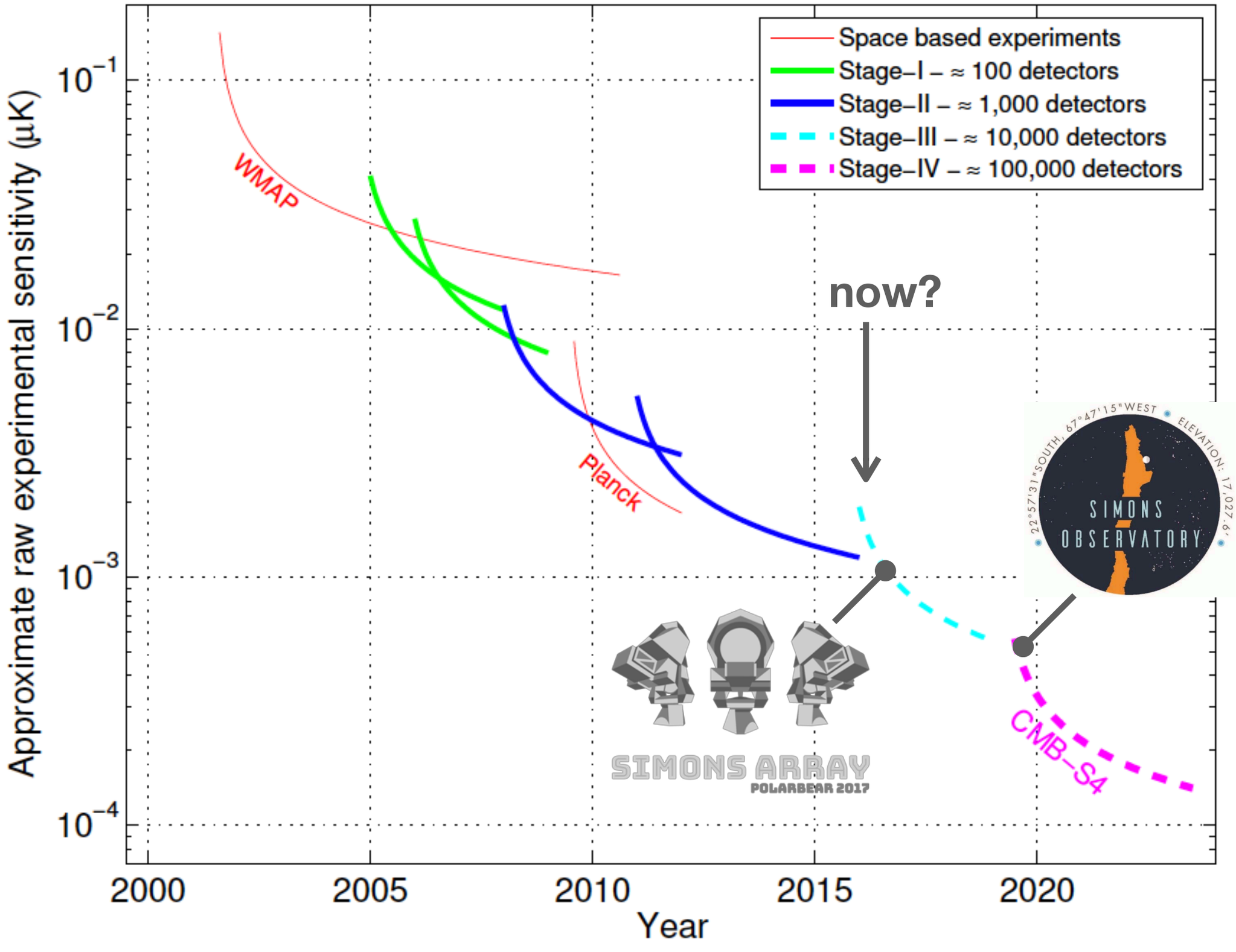

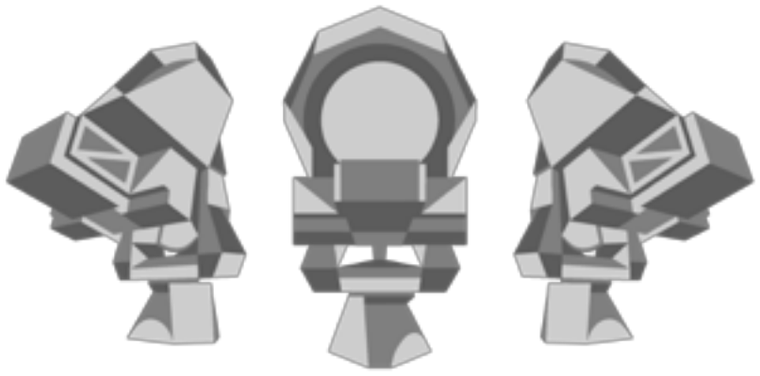

- 22,000 polarization sensitive detectors
- sinuous antennas (dual-frequency-band pixels)
- 4 frequency bands total (95,150,220,280GHz)
- 3.5’ beam @ 150GHz

SIMONS ARRAY
POLARBEAR 2017

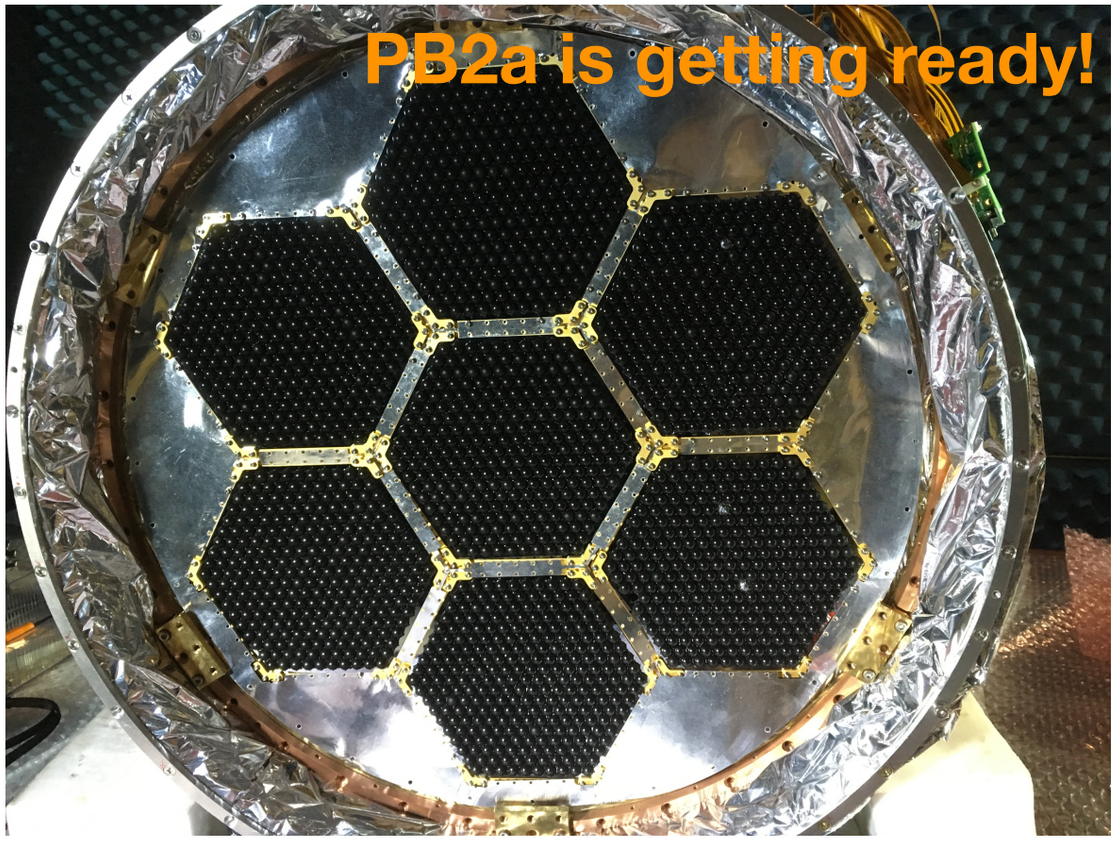

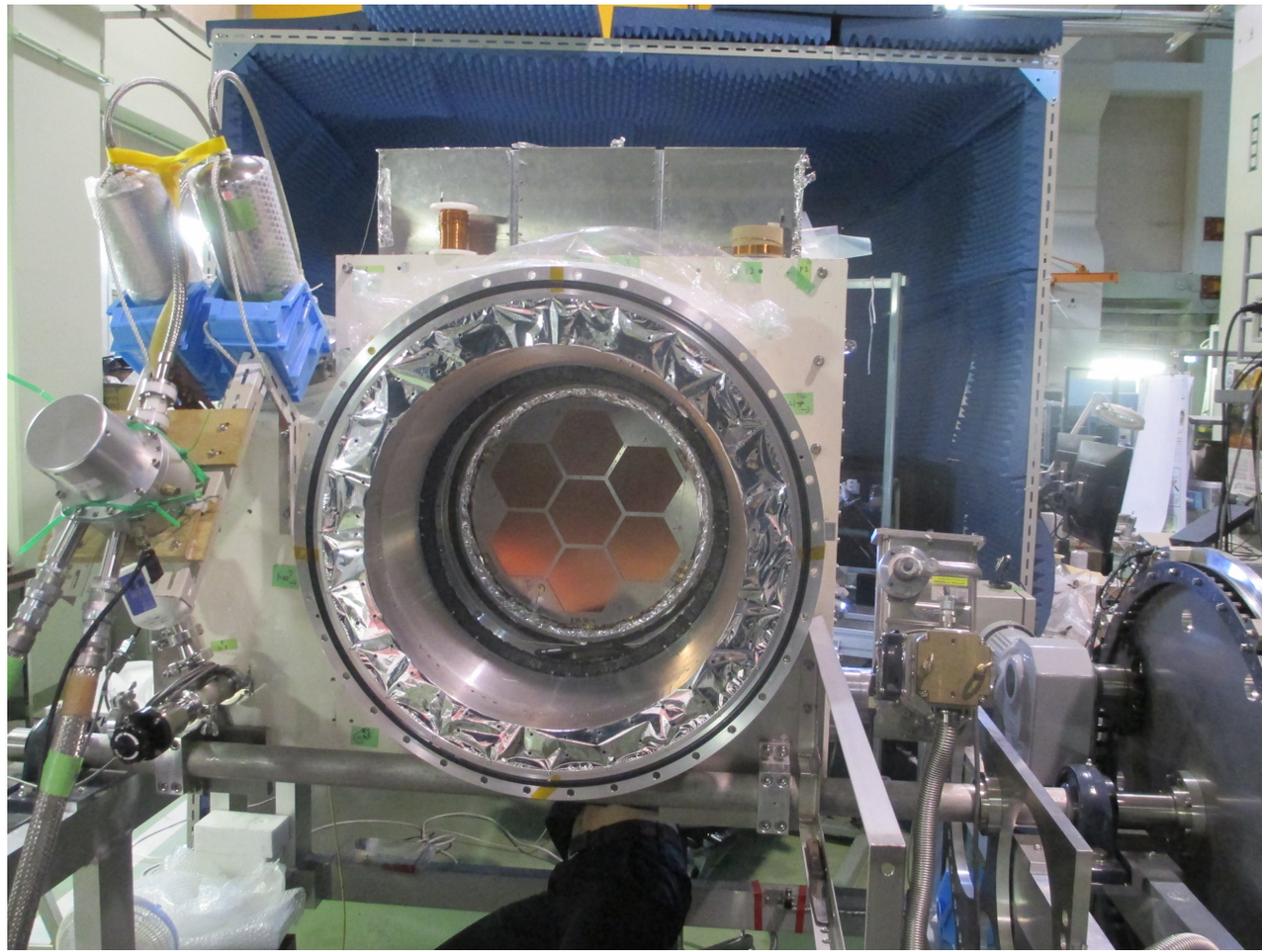

Simons Observatory

- O(80,000) detectors
- deep patch fsky = O(5%) -> inflation
- large patch fsky = O(25%) -> lensing
- small aperture (FWHM = O(.5deg)) and large aperture (FWHM = O(1 arcmin))
- O(7-8) frequency bands between 30 and 280GHz

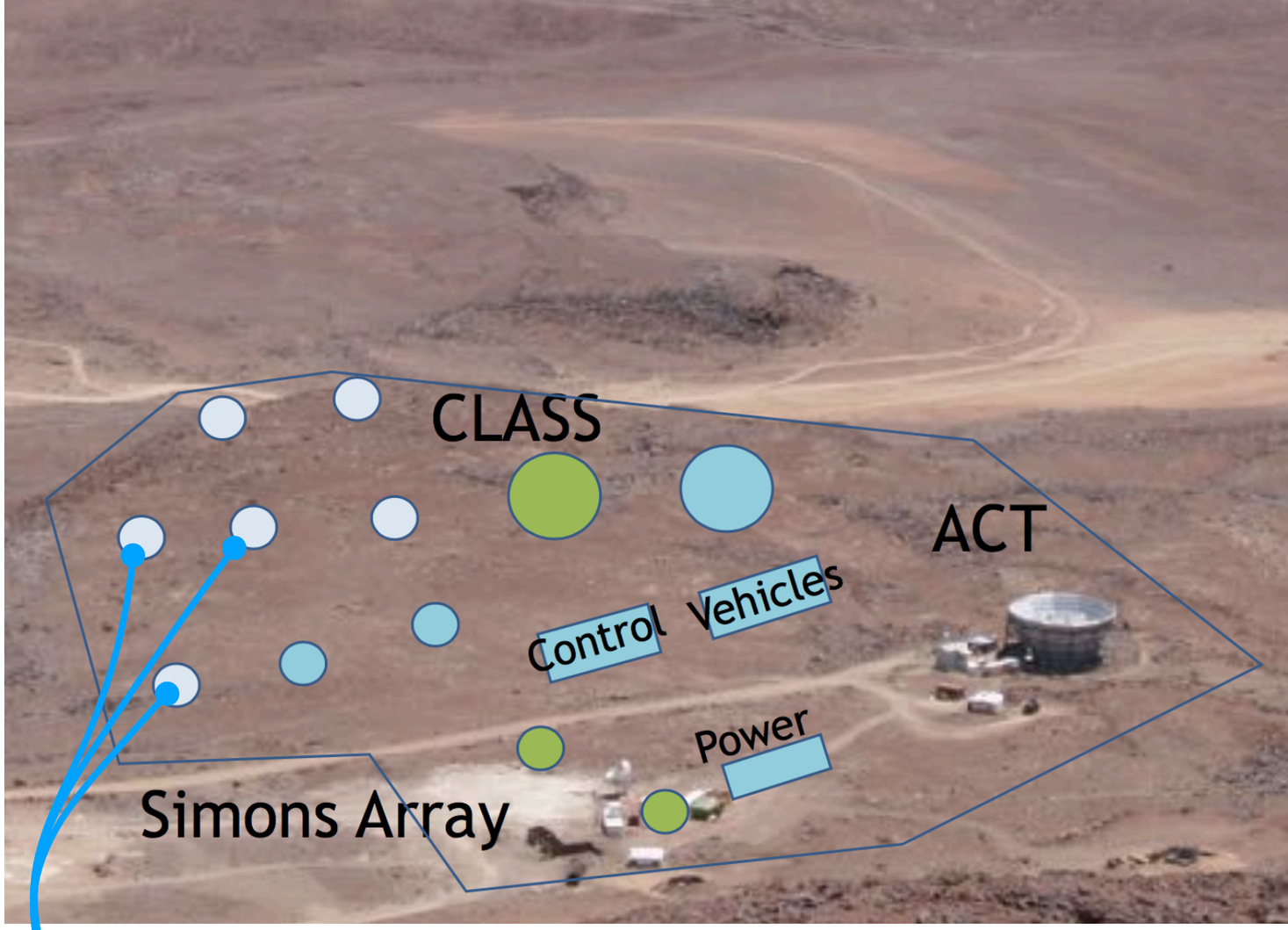

small aperture telescope

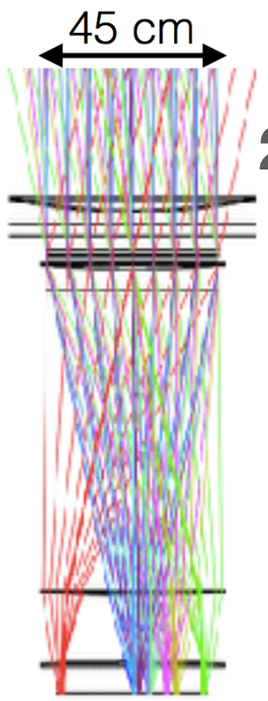

2-refractor setup

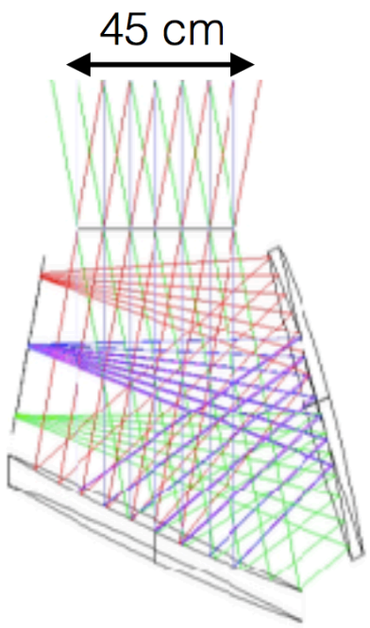

crossed Dragone setup

SIMONS OBSERVATORY

22°57'31"SOUTH, 67°47'15"WEST • ELEVATIO

large aperture telescope

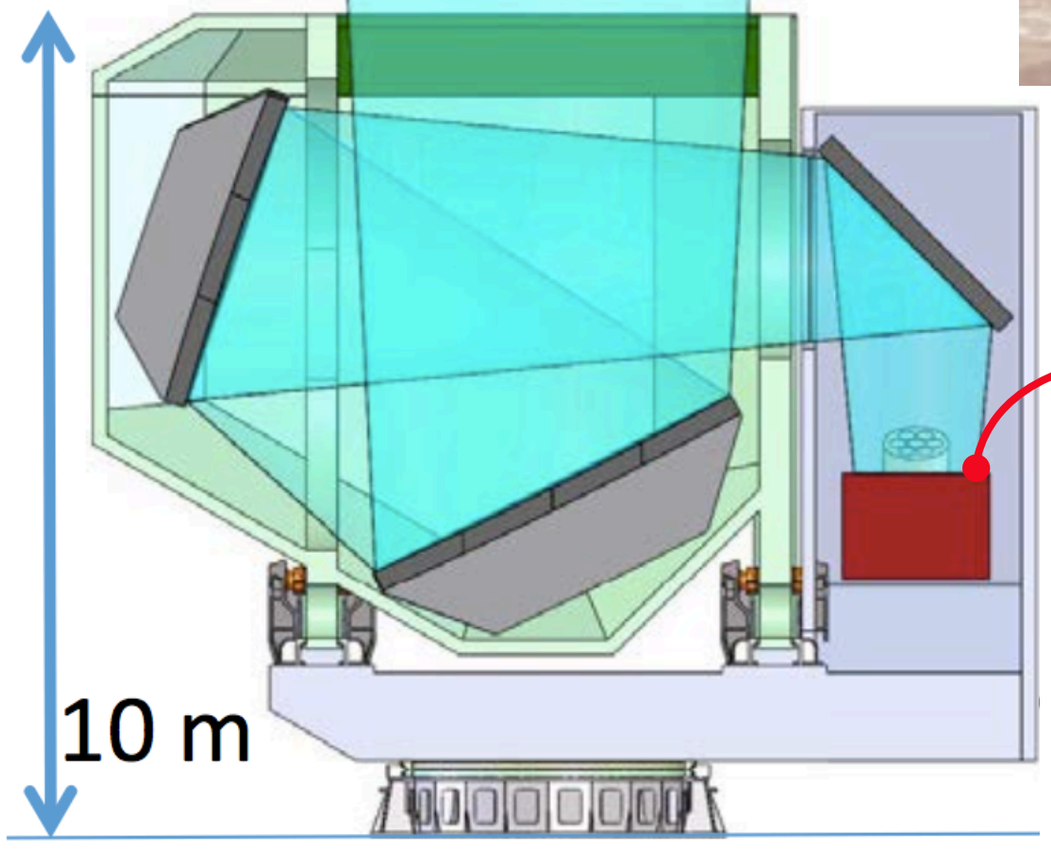

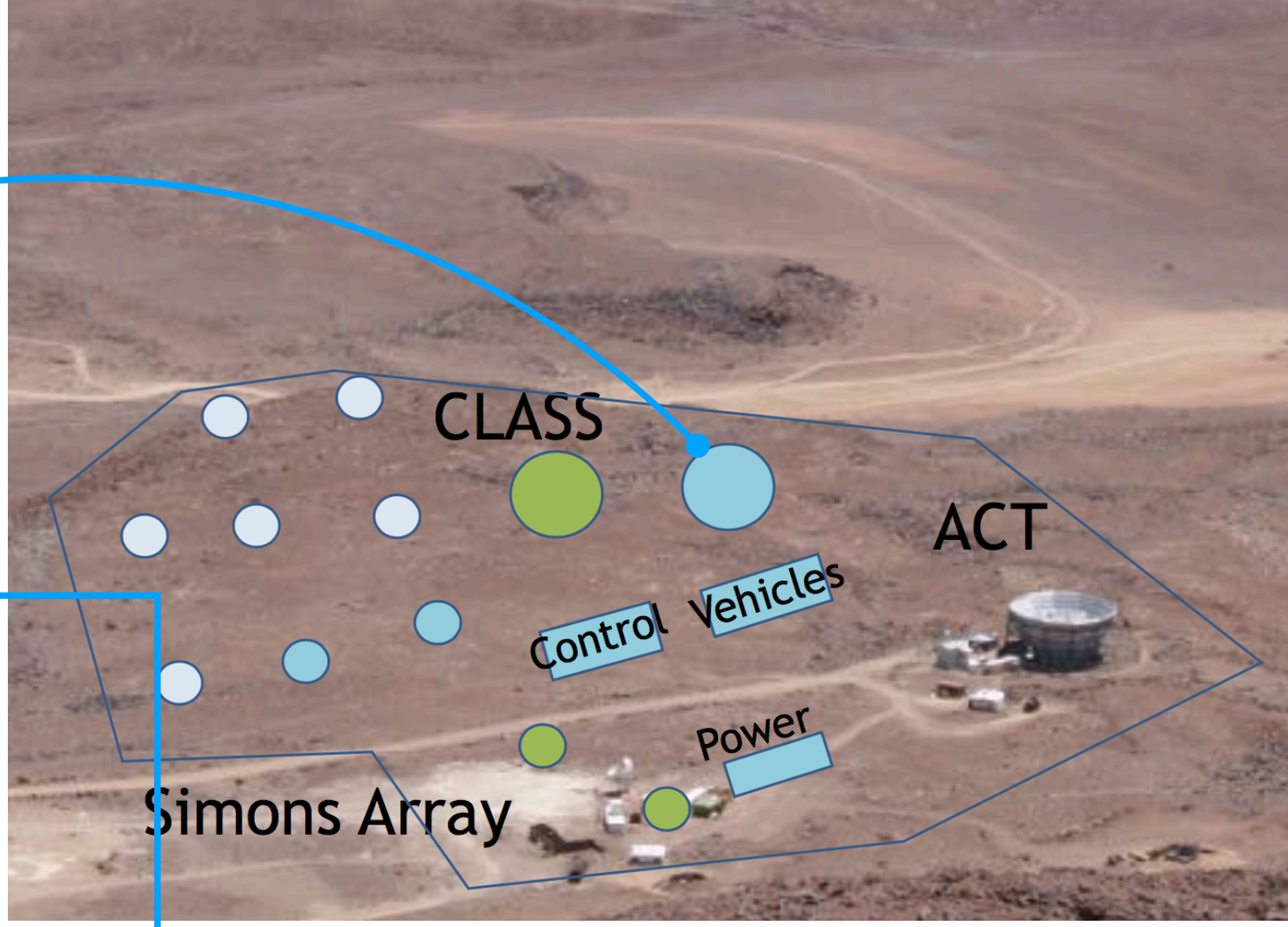

~2 m diameter receiver for each large aperture telescope.

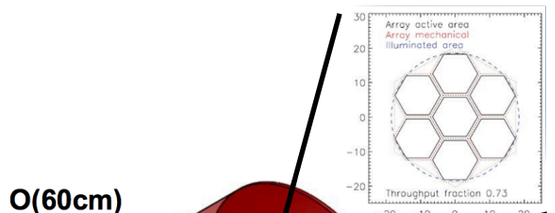

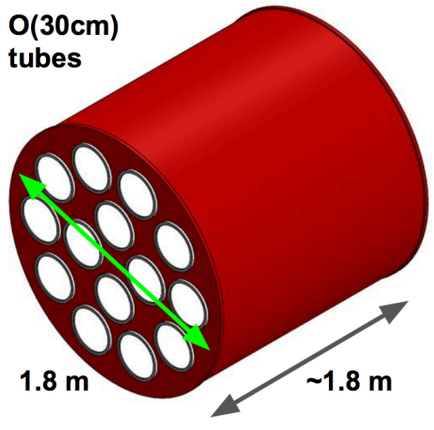

2 -3 O(60cm) Optics tubes per receiver

~14 O(30cm) Optics tubes per receiver

CMB-S4

- One collaboration, one project, with two sites: **South Pole** and **Atacama, Chile**
- Small and large telescopes for **B-mode, delensing, high-l** cosmic structure science
- **500,000 detectors** (300k on 3 large telescopes; 200k on 14 small telescopes)
- Order **8 frequency bands** for CMB and foreground mitigation on small telescopes
- Two surveys:
  - ⋆ 4 yr deep B-mode w/ delensing (f_{sky} ~ few %)
  - ⋆ 7 yr broad for N_{eff} and cosmic structure science (f_{sky} = 40%)

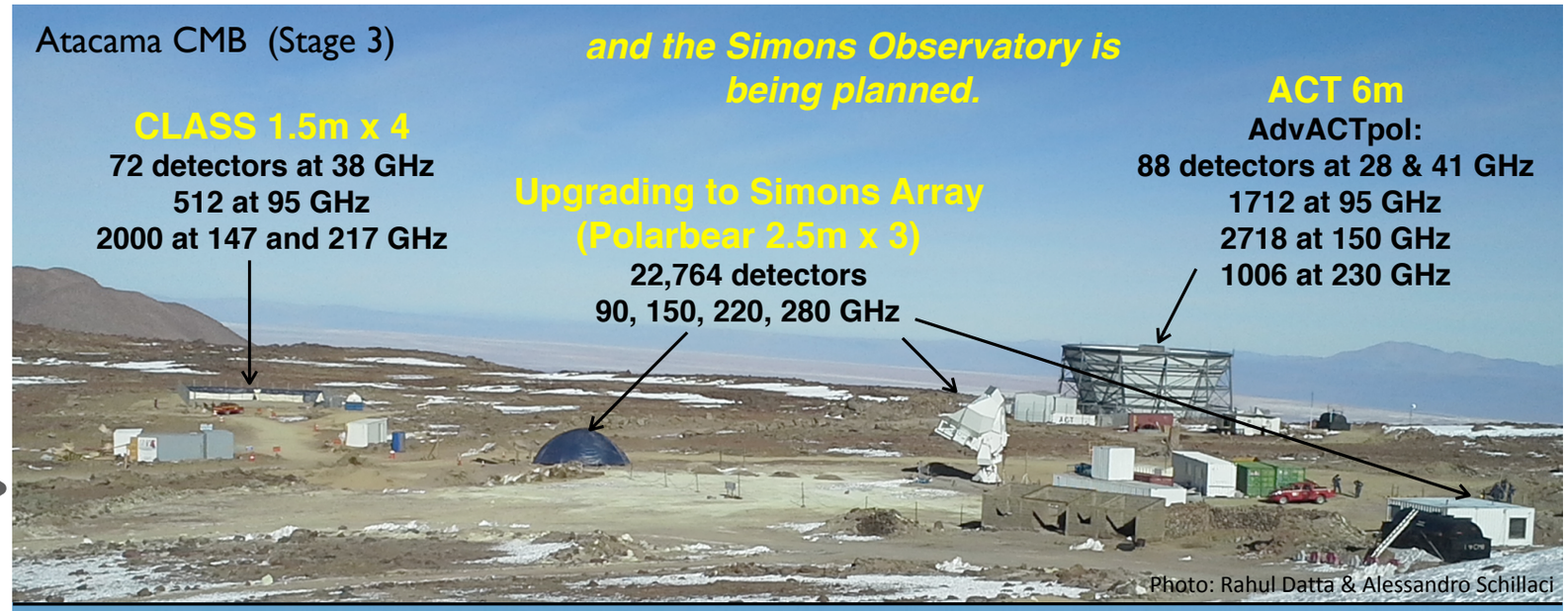

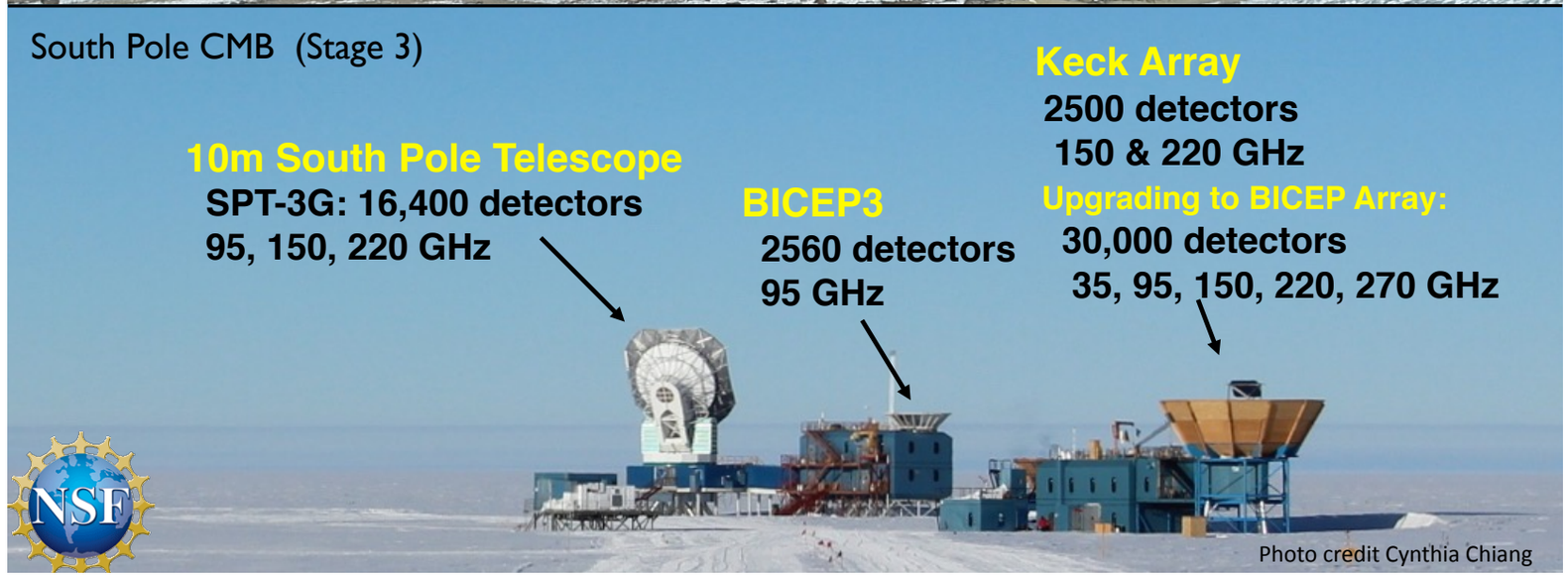

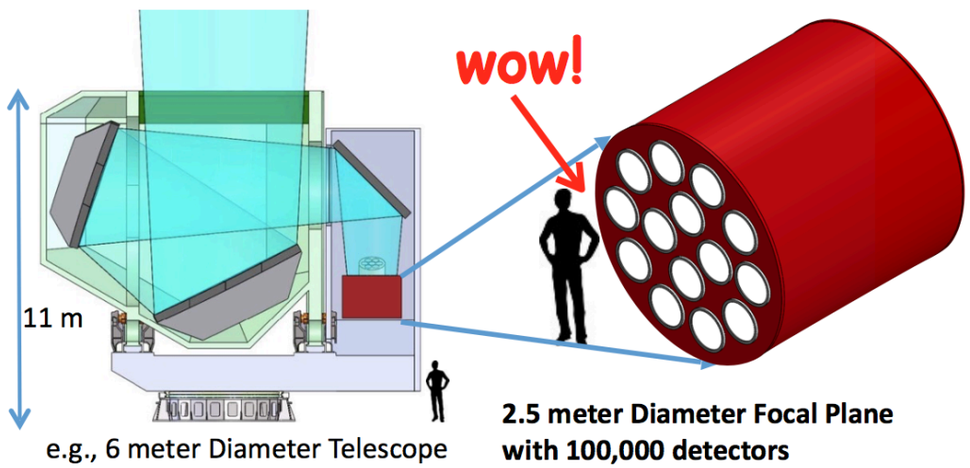

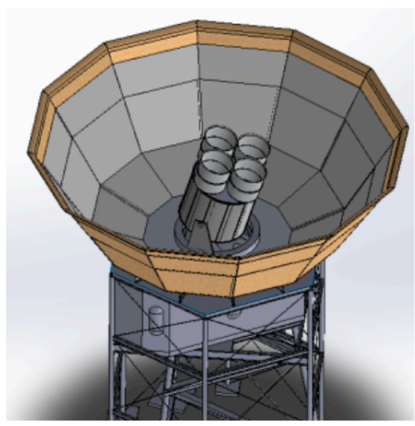

High resolution Science + de-lensing:
300,000 detectors on 3 large telescopes

Low resolution B-mode Science:
200,000 det. on 14 small telescopes

CMB-S4 Science Book, arXiv: 1610.02743

		Sensitivity (μK^2)	$\sigma(r)$	$\sigma(N_{eff})$	$\sigma(\Sigma m_\nu)$	Dark Energy F.O.M
2015	Stage 2 1000 detectors				Boss BAO prior	DES+BOSS SPT clusters
2016		$\gtrsim 10^{-5}$	0.035	0.14	0.15eV	~180
2017	Stage 3 10,000 detectors					
2018						
2019					Boss BAO prior	DES + DESI SZ Clusters
2020		10^{-6}	0.006	0.06	0.06eV	~300-600
2021	Stage 4 CMB-S4 ~500,000 detectors					
2022						
2023					DESI BAO +τ_e prior	DESI +LSST S4 Clusters
Target		**10^{-8}**	**0.0005**	**0.027**	**0.015eV**	**1250**

CMB-S4 Science Book, arXiv: 1610.02743

Dark energy observables:

- cluster abundance and mass
- lensing
- kinematic SZ
- cosmic birefringence

CMB-S4 Science Book, arXiv: 1610.02743

Dark energy observables:

- **cluster abundance and mass**
- **lensing**
- **kinematic SZ**
- **cosmic birefringence**

[see talk by Marian Douspis]

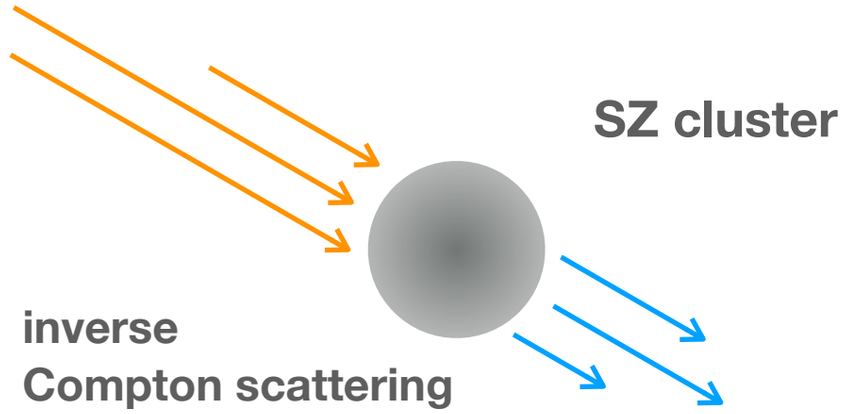

↳ SZ surveys provide relatively clean, nearly mass-limited catalogs of clusters out to the highest redshifts where they exist;
in particular, SZ surveys are easily the most efficient approach to finding massive clusters at $z > 1$.

CMB-S4 Science Book, arXiv: 1610.02743

Dark energy observables:

- **cluster abundance and mass**
- **lensing**
- **kinematic SZ**
- **cosmic birefringence**

[see talk by Marian Douspis]

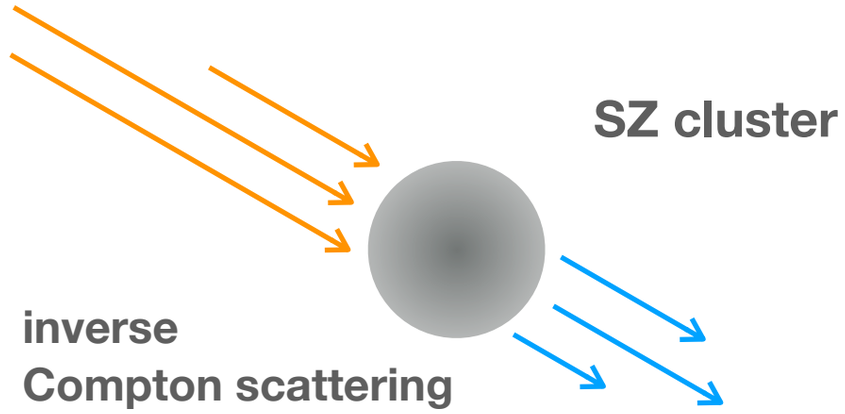

↳ SZ surveys provide relatively clean, nearly mass-limited catalogs of clusters out to the highest redshifts where they exist;
in particular, SZ surveys are easily the most efficient approach to finding massive clusters at z > 1.

FHWM ↘, cost ↗, mass threshold ↘, # of detected clusters ↗ (especially at high redshifts)

CMB-S4 Science Book, arXiv: 1610.02743

Dark energy observables:

- **cluster abundance and mass**
- **lensing**
- **kinematic SZ**
- **cosmic birefringence**

[see talk by Marian Douspis]

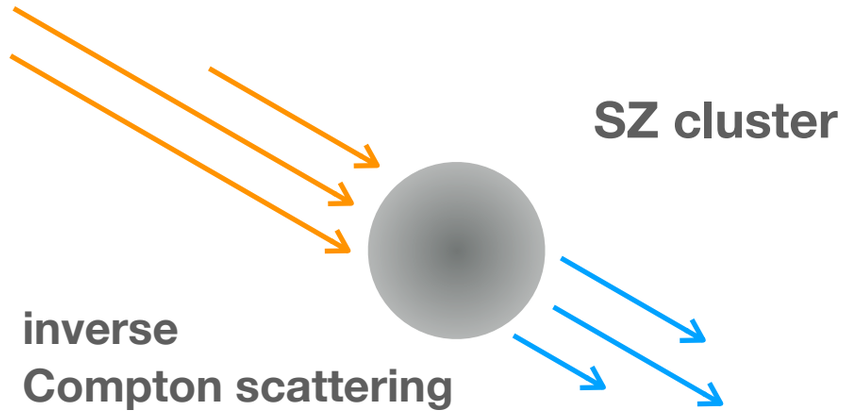

SZ surveys provide relatively clean, nearly mass-limited catalogs of clusters out to the highest redshifts where they exist;
in particular, SZ surveys are easily the most efficient approach to finding massive clusters at z > 1.

FHWM ↘, cost ↗, mass threshold ↘, # of detected clusters ↗ (especially at high redshifts)

relative mass calibration with X-ray observations (Chandra, XMM-Newton, eROSITA, ATHENA)	**absolute mass calibration with lensing** (galaxy cluster weak lensing, CMB lensing at high redshifts)

CMB-S4 Science Book, arXiv: 1610.02743

Dark energy observables:

- **cluster abundance and mass**
- **lensing**
- **kinematic SZ**
- **cosmic birefringence**

[see talk by Marian Douspis]

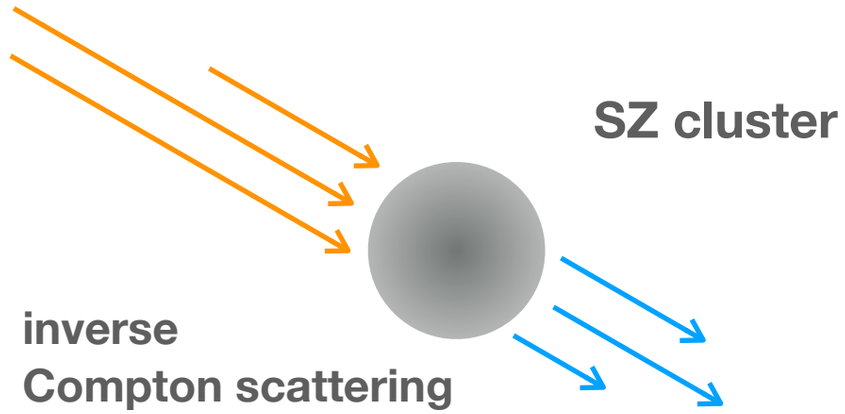

SZ surveys provide relatively clean, nearly mass-limited catalogs of clusters out to the highest redshifts where they exist;
in particular, SZ surveys are easily the most efficient approach to finding massive clusters at z > 1.

FHWM ↘, cost ↗, mass threshold ↘, # of detected clusters ↗ (especially at high redshifts)

relative mass calibration with X-ray observations (Chandra, XMM-Newton, eROSITA, ATHENA)

absolute mass calibration with lensing (galaxy cluster weak lensing, CMB lensing at high redshifts)

50% mass completeness limits

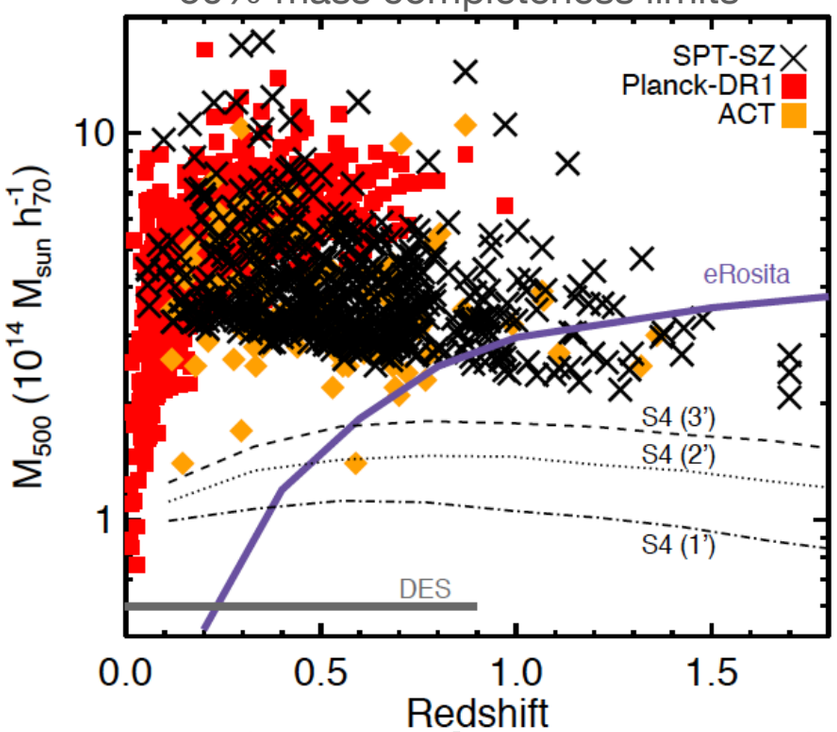

projected cluster counts

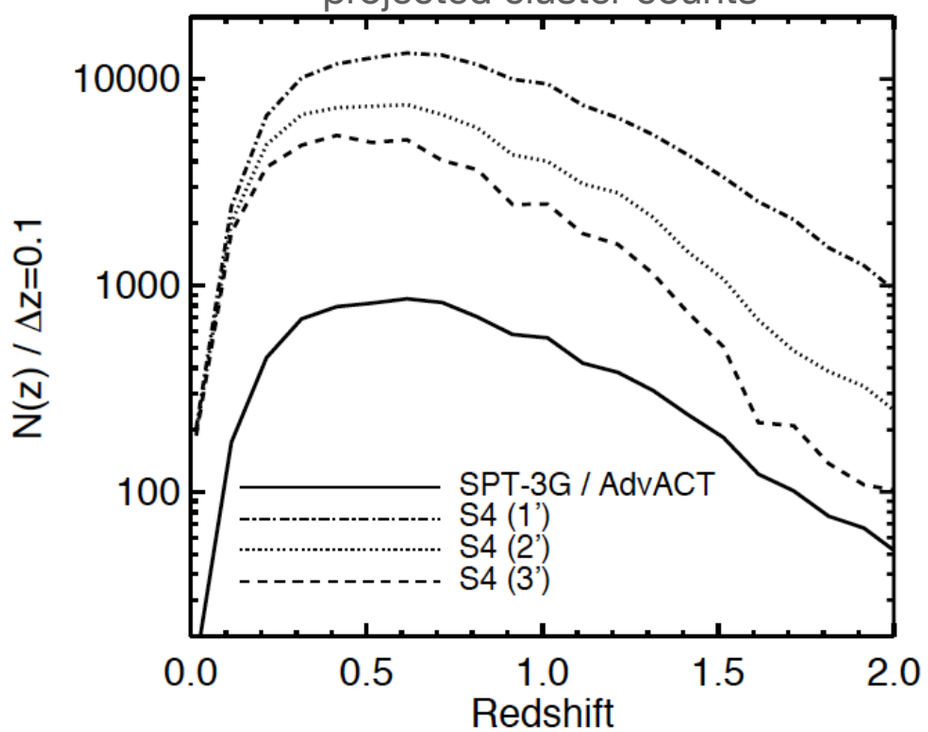

great complement to DESI and LSST and Euclid

CMB-S4 Science Book, arXiv: 1610.02743

Dark energy observables:

- cluster abundance and mass
- lensing
- kinematic SZ
- cosmic birefringence

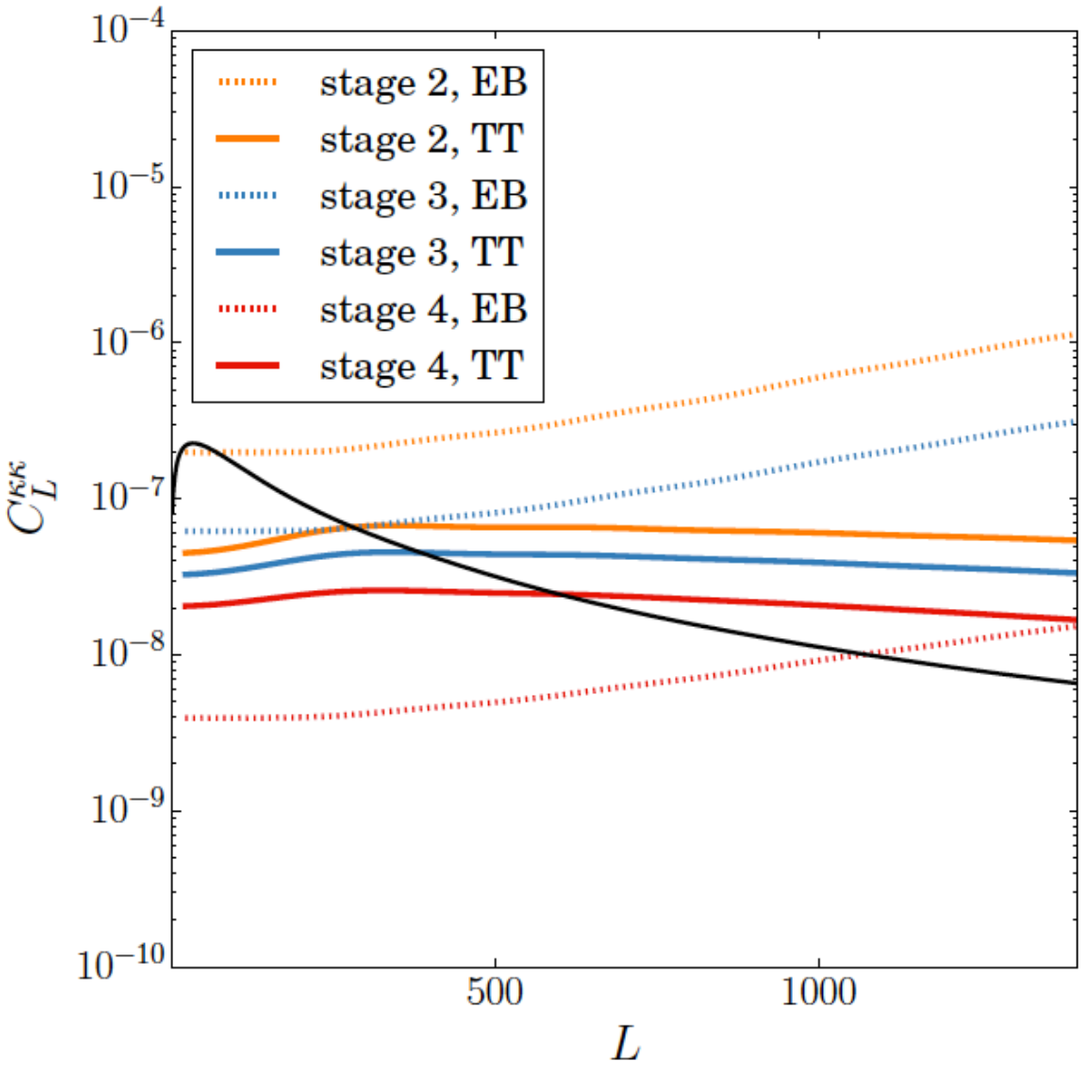

Figure 46. *Signal and noise-per-mode curves for three experiments. "Stage 2" is meant to represent a current-generation survey like SPTpol or ACTPol and has $\Delta_T = 9\mu$K-arcmin; "Stage 3" is an imminent survey like SPT-3G or AdvACT, with $\Delta_T = 5\mu$K-arcmin; and "Stage 4" has a nominal noise level of $\Delta_T = 1\mu$K-arcmin. These noise-per-mode curves do not depend on the area of sky surveyed. All experiments assume a 1.'0 beam, and a maximum l of 5000.*

CMB-S4 Science Book, arXiv: 1610.02743

Dark energy observables:

- cluster abundance and mass
- lensing
- kinematic SZ
- cosmic birefringence

Figure 49. *Constraining neutrino mass with CMB-S4. Top: lensing power spectra for multiple neutrino masses (curves) together with forecasted errors for S4. Bottom: residual from curve at zero neutrino mass. Error boxes are shown centered at the minimal value of 60 meV. S4 will be targeted to resolve differences in neutrino mass of 20 meV.*

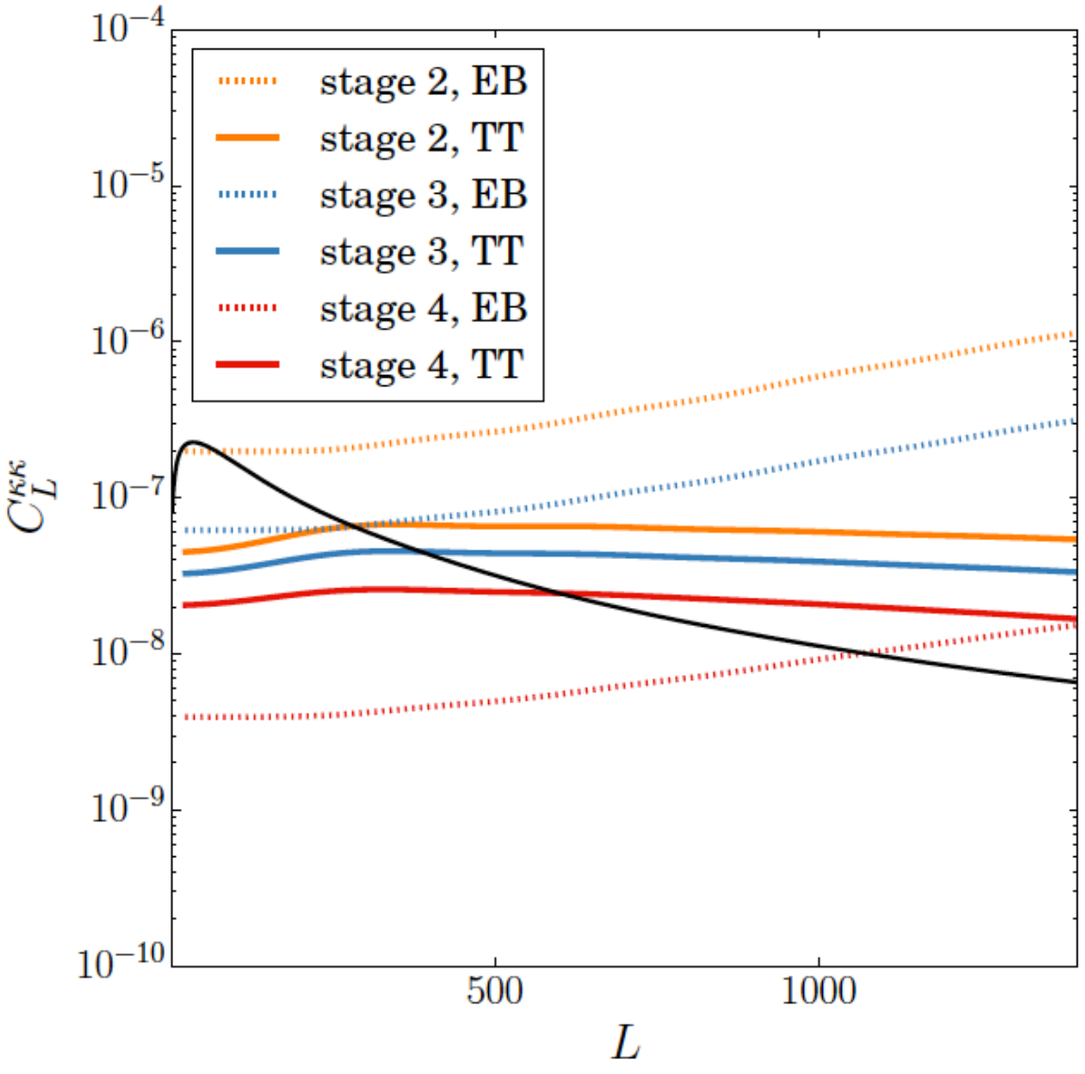

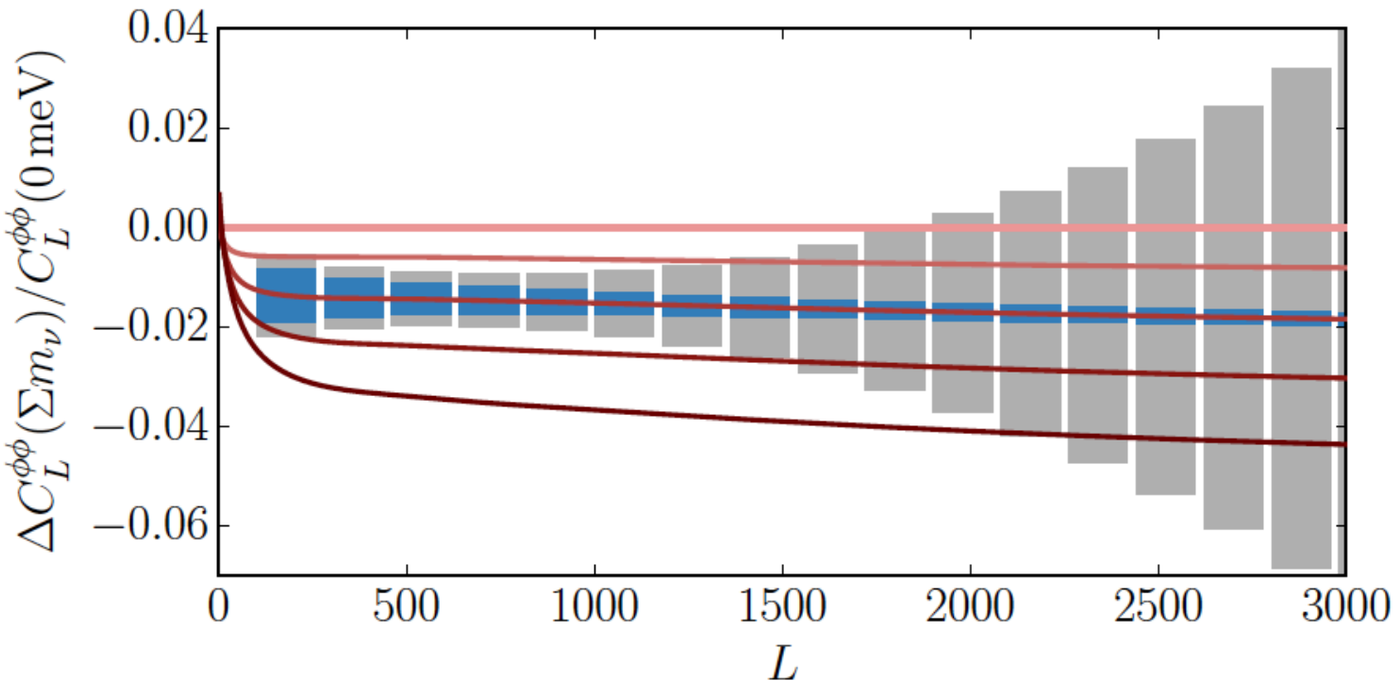

[see talk by Olivier Perdereau]

Figure 46. *Signal and noise-per-mode curves for three experiments. "Stage 2" is meant to represent a current-generation survey like SPTpol or ACTPol and has $\Delta_T = 9\mu$K-arcmin; "Stage 3" is an imminent survey like SPT-3G or AdvACT, with $\Delta_T = 5\mu$K-arcmin; and "Stage 4" has a nominal noise level of $\Delta_T = 1\mu$K-arcmin. These noise-per-mode curves do not depend on the area of sky surveyed. All experiments assume a 1.'0 beam, and a maximum l of 5000.*

CMB-S4 Science Book, arXiv: 1610.02743

Dark energy observables:

- cluster abundance and mass
- lensing
- **kinematic SZ**
- cosmic birefringence

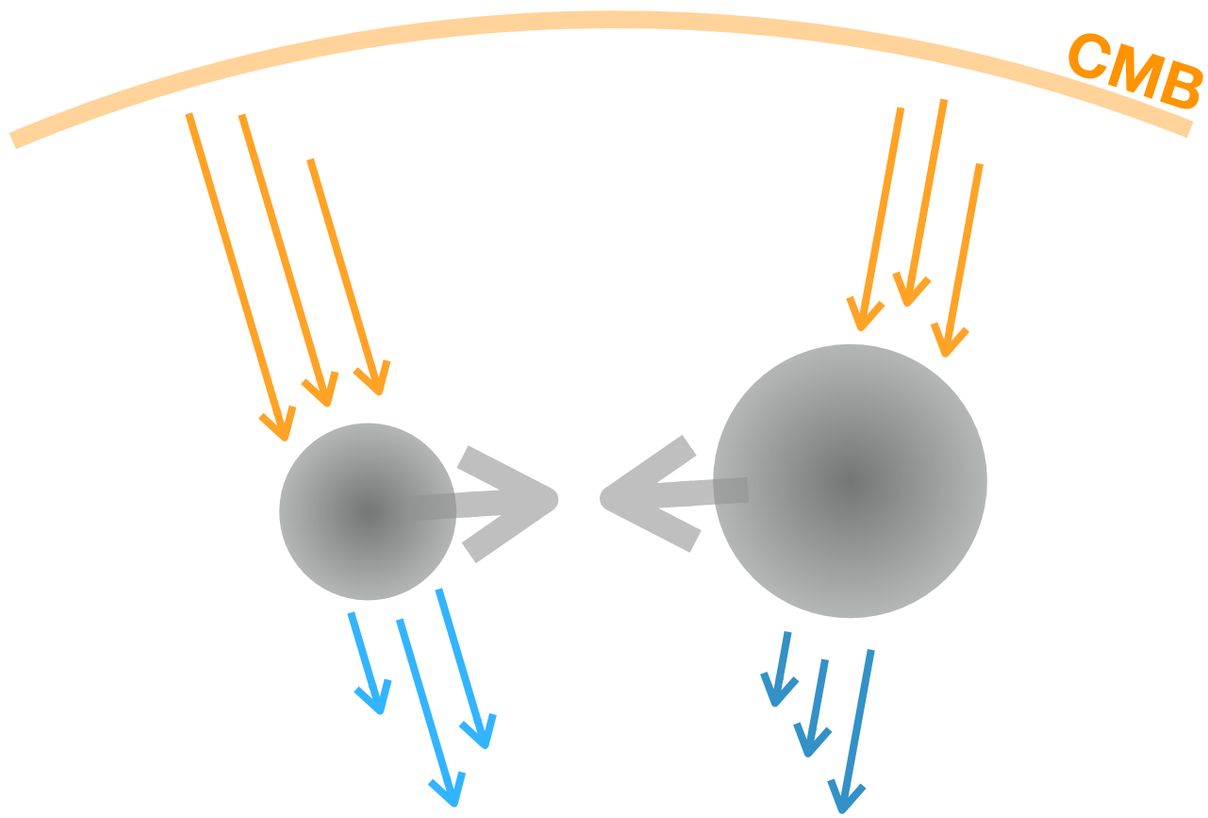

- multi-frequency data can be used to remove other foregrounds and isolate kSZ signal
- CMB-S4 will enable sub-percent precision measurements of the matter density σ_8 fluctuations through the diffuse kSZ anisotropy ➔ test for ΛCDM
- patchy kSZ ➔ reionization
- mean pairwise velocity is sensitive to both the growth of structure and the expansion history of the Universe ; excellent probe for gravity on large scales ➔ e.g. w, neutrino mass

Figure 39. *kSZ S/N for different beam FWHM and noise level between 1 μK-arcmin (top curve) to 9 μK-arcmin (bottom curve) for a DESI-like spectroscopic galaxy survey, using the "velocity reconstruction" or "pairwise momentum" techniques.*

CMB-S4 Science Book, arXiv: 1610.02743

Dark energy observables:

- **cluster abundance and mass**
- **lensing**
- **kinematic SZ**
- **cosmic birefringence**

- multi-frequency data can be used to remove other foregrounds and isolate kSZ signal
- CMB-S4 will enable sub-percent precision measurements of the matter density σ_8 fluctuations through the diffuse kSZ anisotropy ➔ test for ΛCDM
- patchy kSZ ➔ reionization
- mean pairwise velocity is sensitive to both the growth of structure and the expansion history of the Universe ; excellent probe for gravity on large scales ➔ e.g. w, neutrino mass

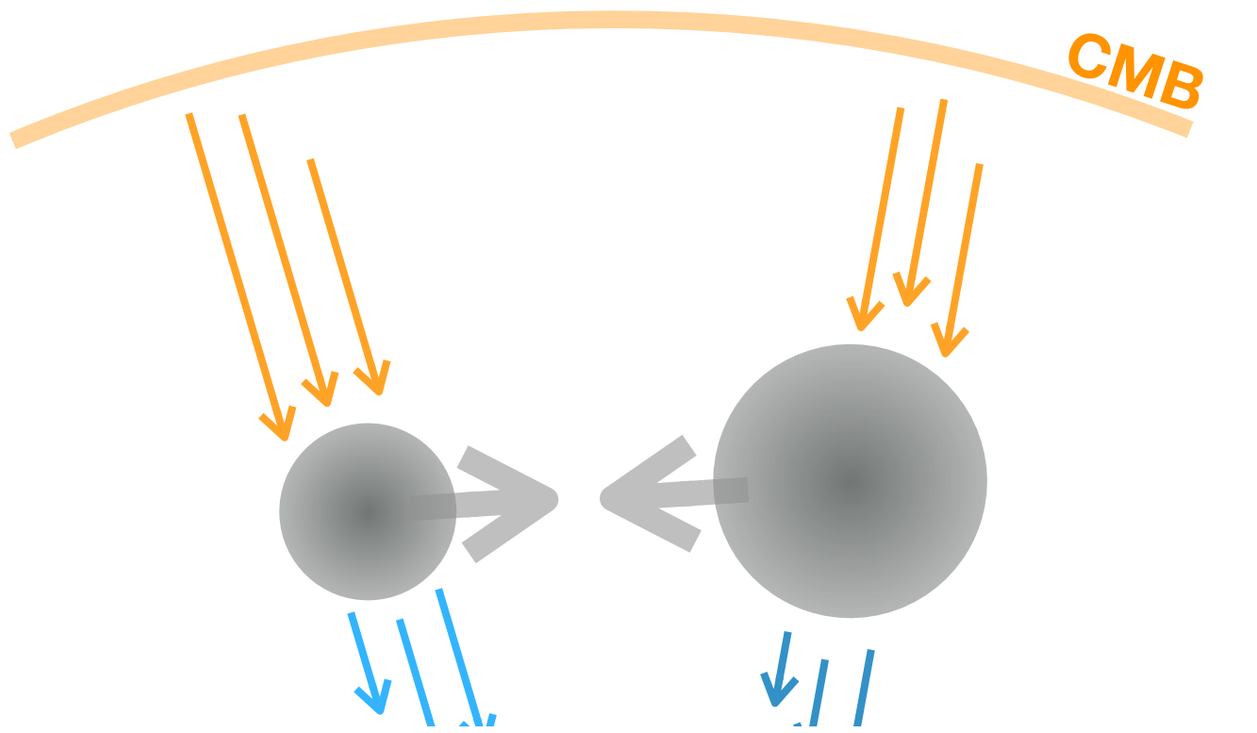

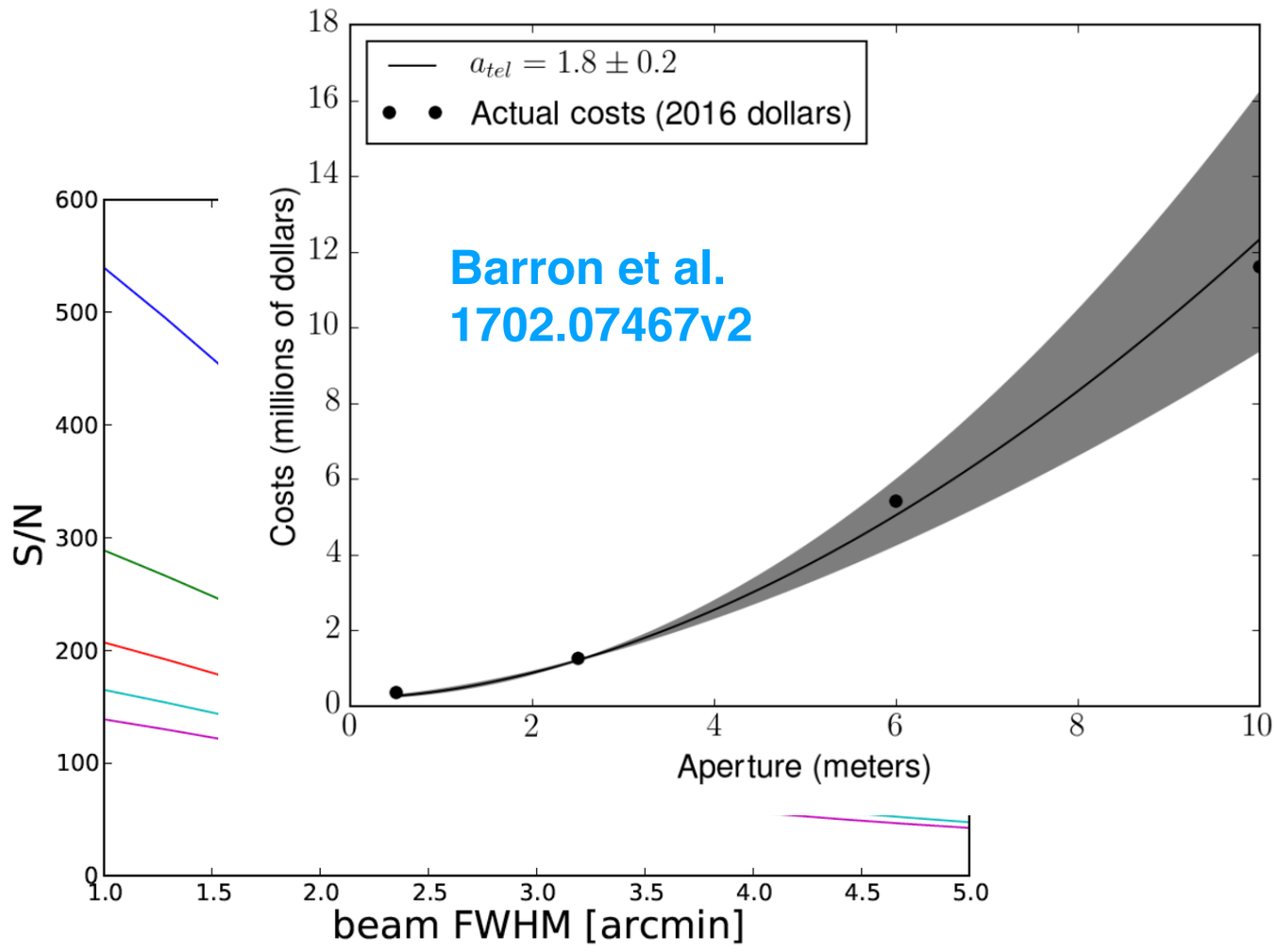

Figure 39. *kSZ S/N for different beam FWHM and noise level between 1 μK-arcmin (top curve) to 9 μK-arcmin (bottom curve) for a DESI-like spectroscopic galaxy survey, using the "velocity reconstruction" or "pairwise momentum" techniques.*

CMB-S4 Science Book, arXiv: 1610.02743

Dark energy observables:

- cluster abundance and mass
- lensing
- kinematic SZ
- **cosmic birefringence**

Coupling between scalar field and photons through the Chern-Simons term in the electromagnetic Lagrangian

$$\mathcal{L} = -\frac{\beta}{4M}\phi F_{\mu\nu}\tilde{F}^{\mu\nu} - V(\phi)$$

$$\alpha = \frac{\beta}{4M}\Delta\phi$$

$$Q' \pm iU' = e^{\pm 2i\alpha}(Q \pm iU)$$

$$C_\ell^{\prime TB} = 2\alpha(\hat{\boldsymbol{n}})C_\ell^{TE}$$
$$C_\ell^{\prime EB} = 2\alpha(\hat{\boldsymbol{n}})C_\ell^{EE}$$

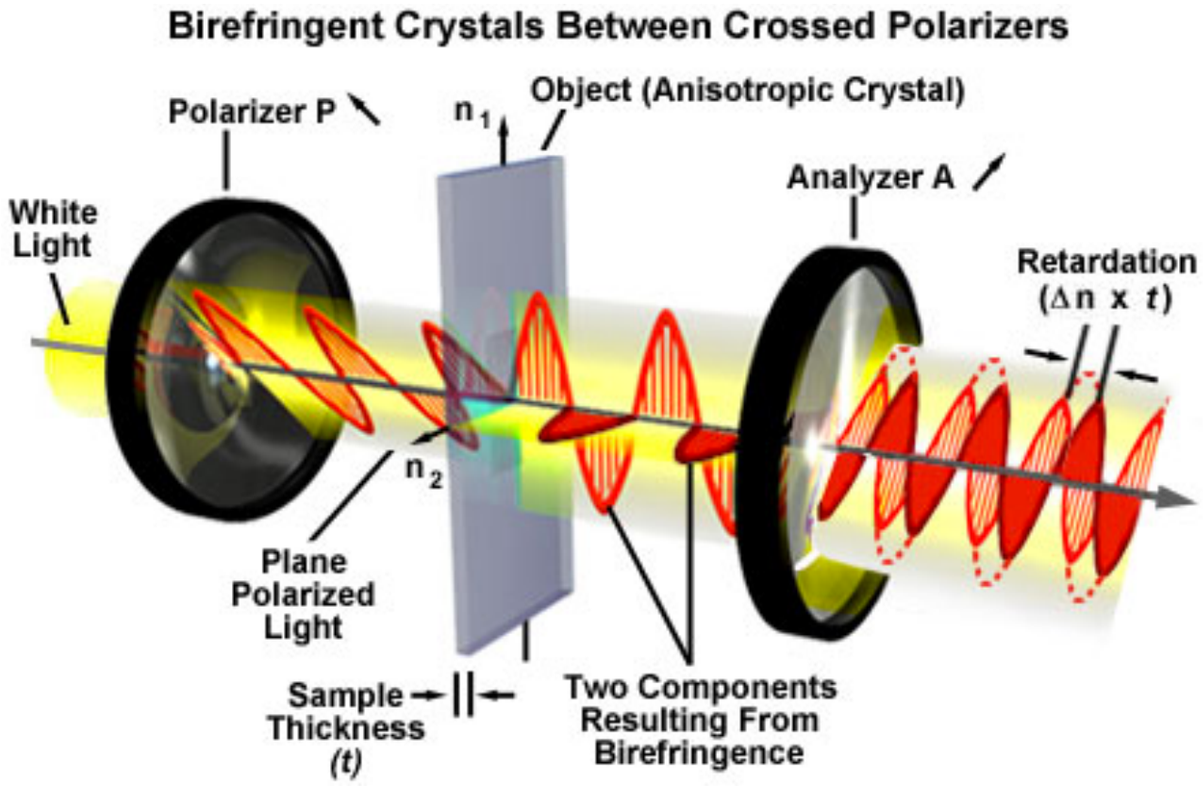

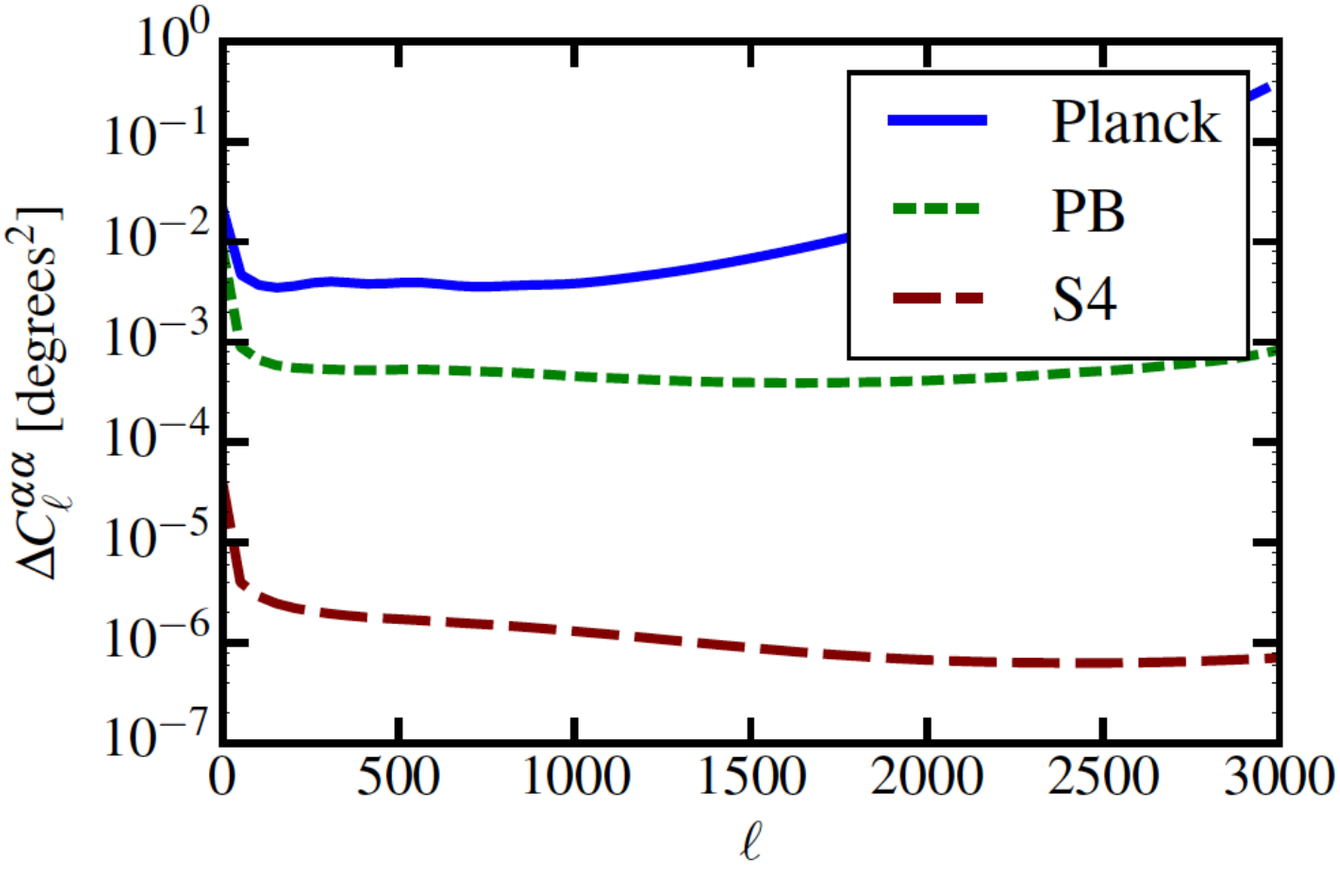

CMB-S4 Science Book, arXiv: 1610.02743

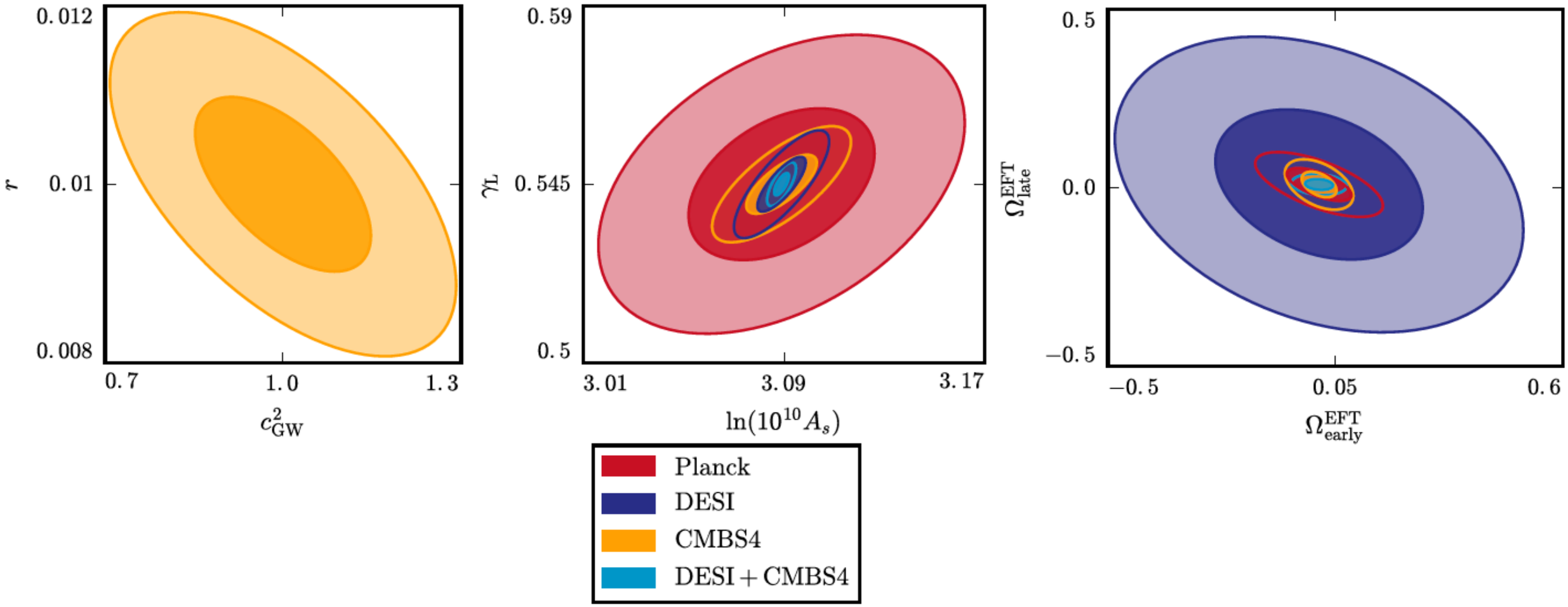

Figure 42. *Forecast marginalized constraints on different models. The left panel shows the joint constraints on the tensor to scalar ratio and the speed of gravitational waves. The central panel shows the joint constraints on the growth index and the amplitude of scalar perturbations. The right panel shows the joint constraints on relative variations of the gravitational constant at early times* $\Omega_0^{\rm EFT}$ *and late times* $\Omega_1^{\rm EFT}$*. Different colors correspond to different experiments, as shown in legend. The darker and lighter shades correspond respectively to the 68% C.L. and the 95% C.L. regions.*

CMB-S4 Science Book, arXiv: 1610.02743

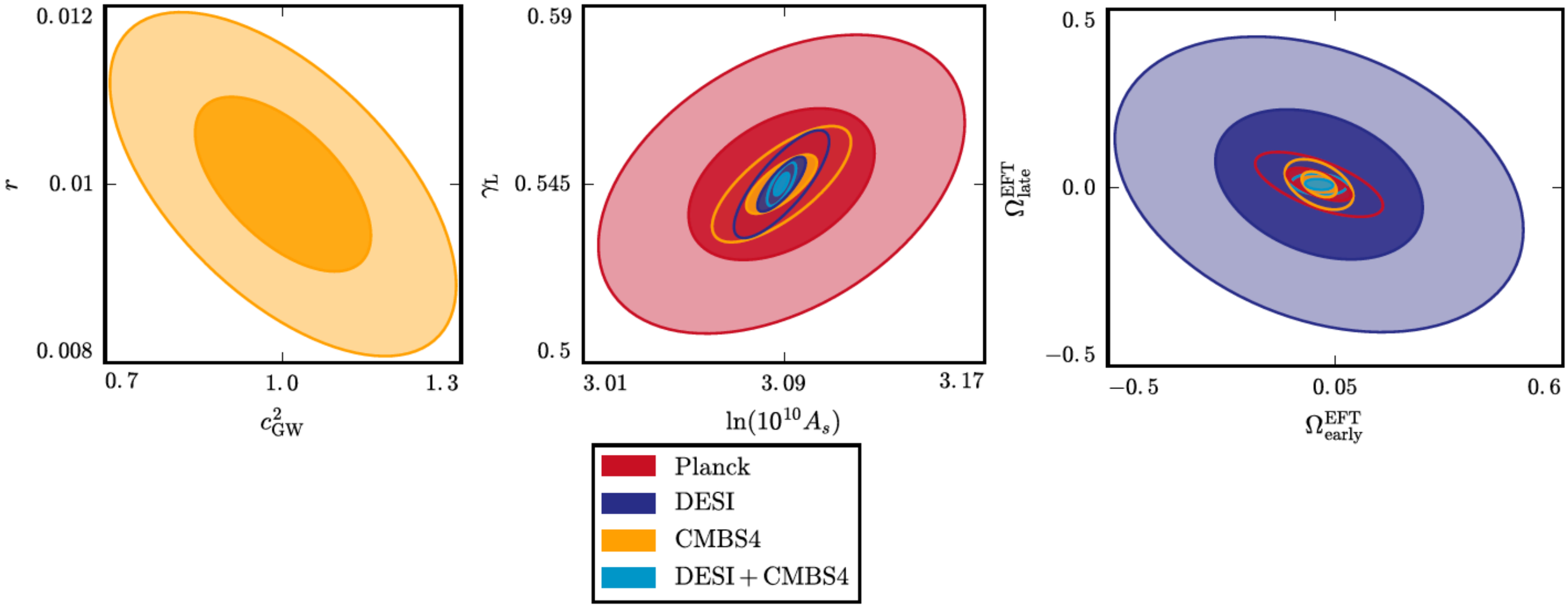

Figure 42. *Forecast marginalized constraints on different models. The left panel shows the joint constraints on the tensor to scalar ratio and the speed of gravitational waves. The central panel shows the joint constraints on the growth index and the amplitude of scalar perturbations. The right panel shows the joint constraints on relative variations of the gravitational constant at early times* $\Omega_0^{\rm EFT}$ *and late times* $\Omega_1^{\rm EFT}$*. Different colors correspond to different experiments, as shown in legend. The darker and lighter shades correspond respectively to the 68% C.L. and the 95% C.L. regions.*

➤ **combination between probes can go a step further …**

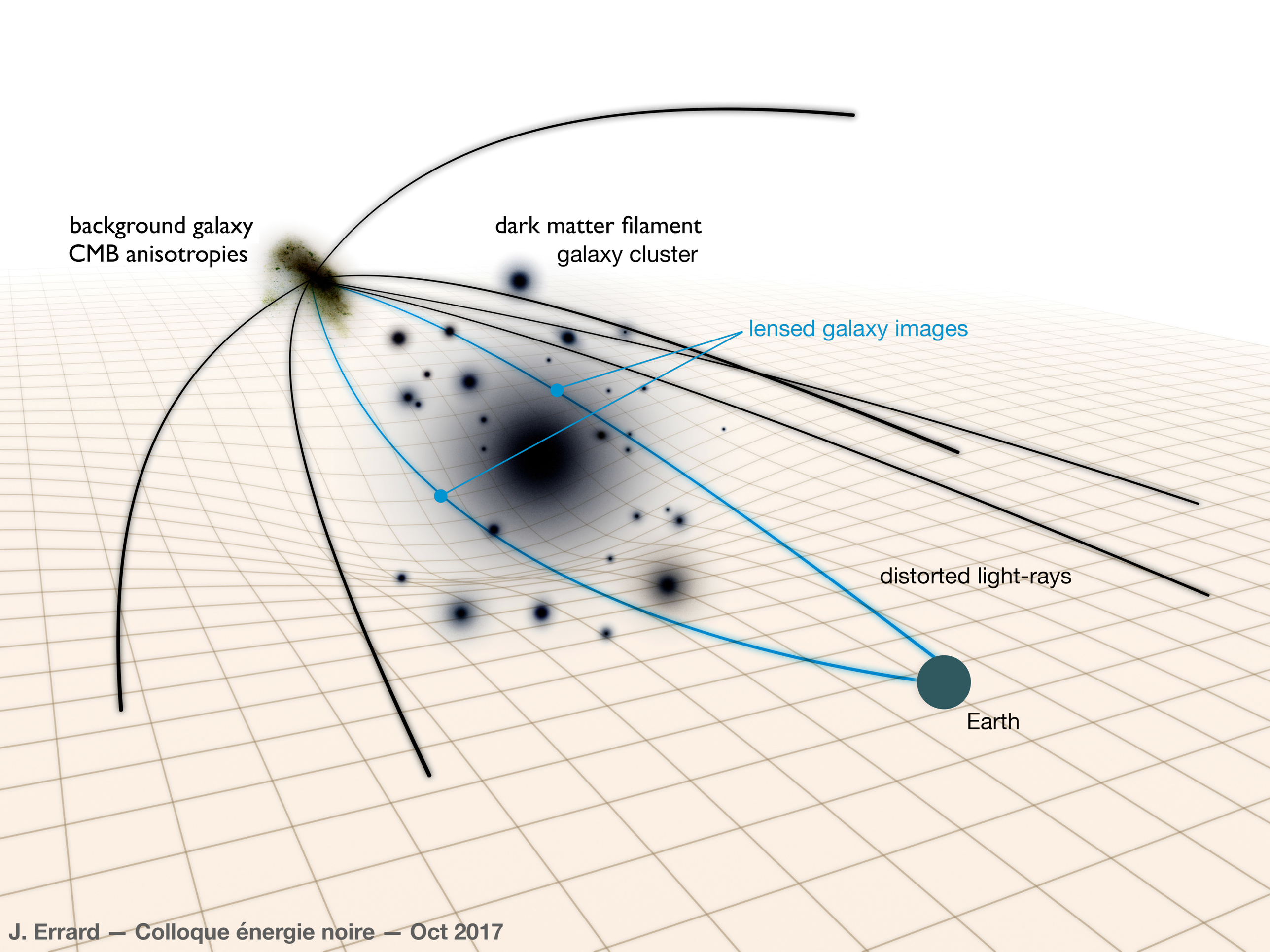
background galaxy
CMB anisotropies
dark matter filament
galaxy cluster
lensed galaxy images
distorted light-rays
Earth

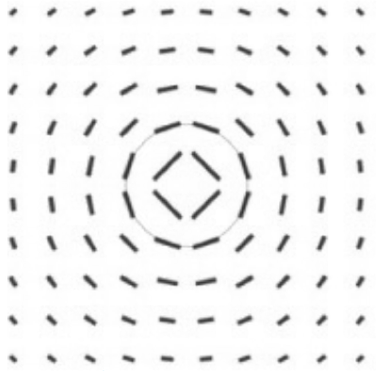

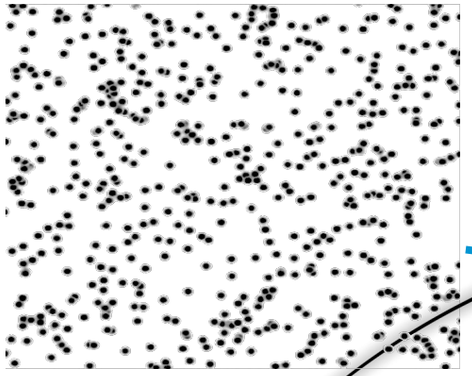

background galaxy
CMB anisotropies

dark matter filament
galaxy cluster

lensed galaxy images

distorted light-rays

Earth

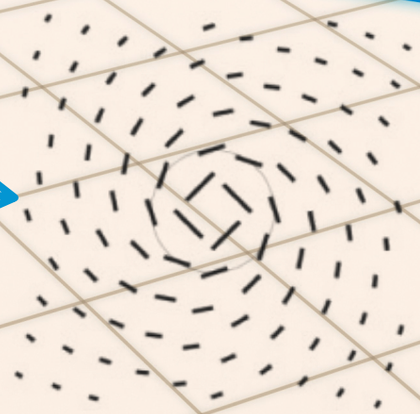

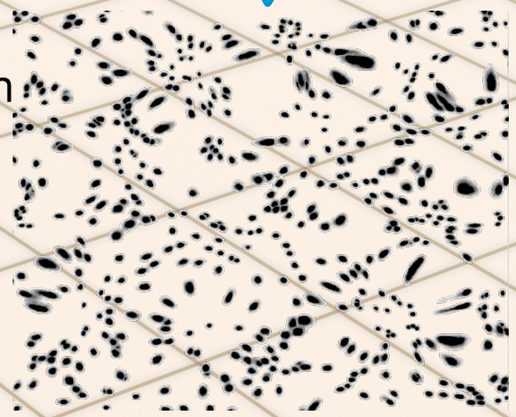

Das, Errard, Spergel arXiv: 1311.2338
Schaan et al. arXiv: 1607.01761

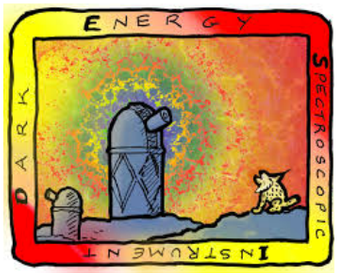

CMB-S4

euclid

LSST
Large Synoptic Survey Telescope

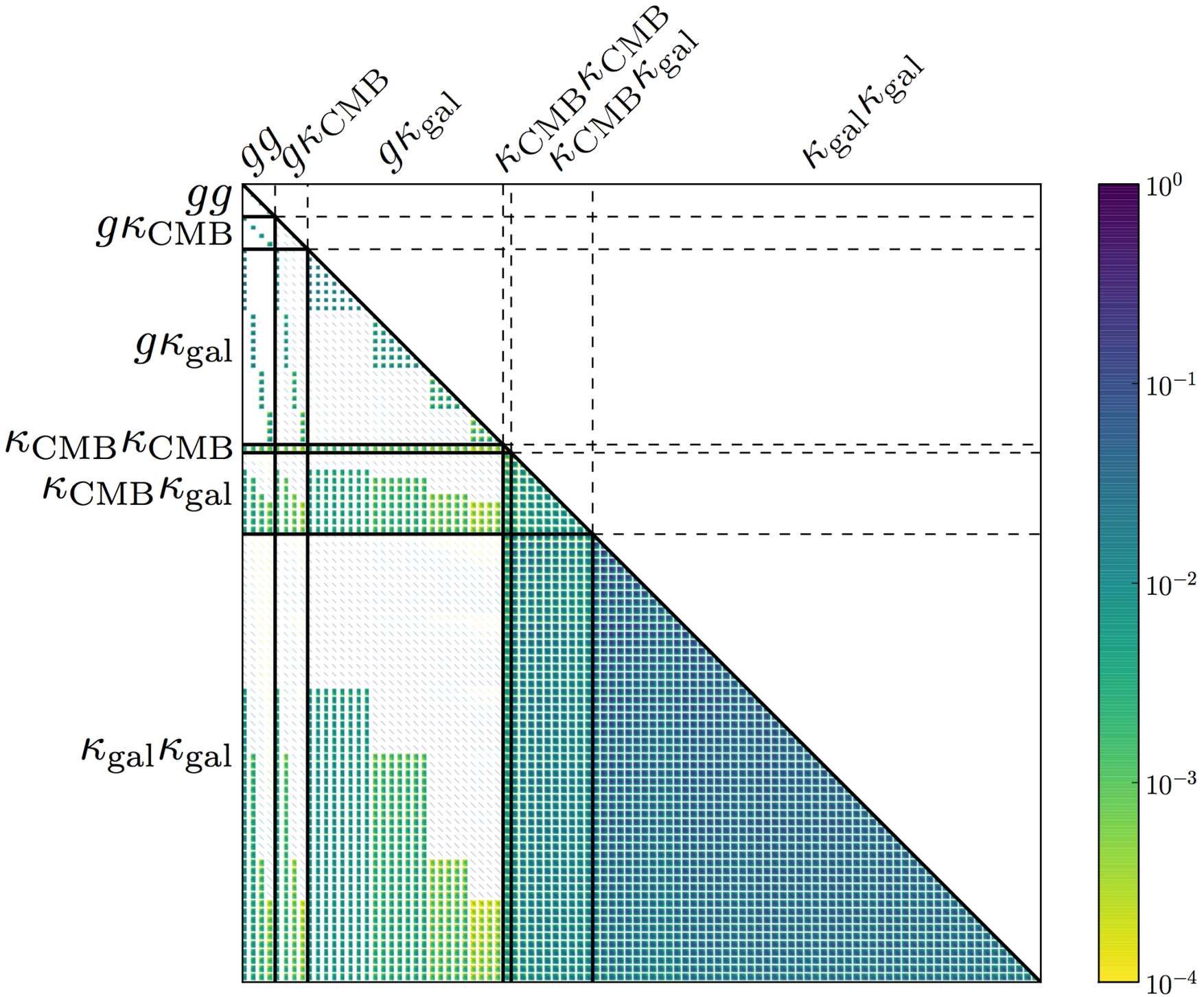

Das, Errard, Spergel arXiv: 1311.2338
Schaan et al. arXiv: 1607.01761

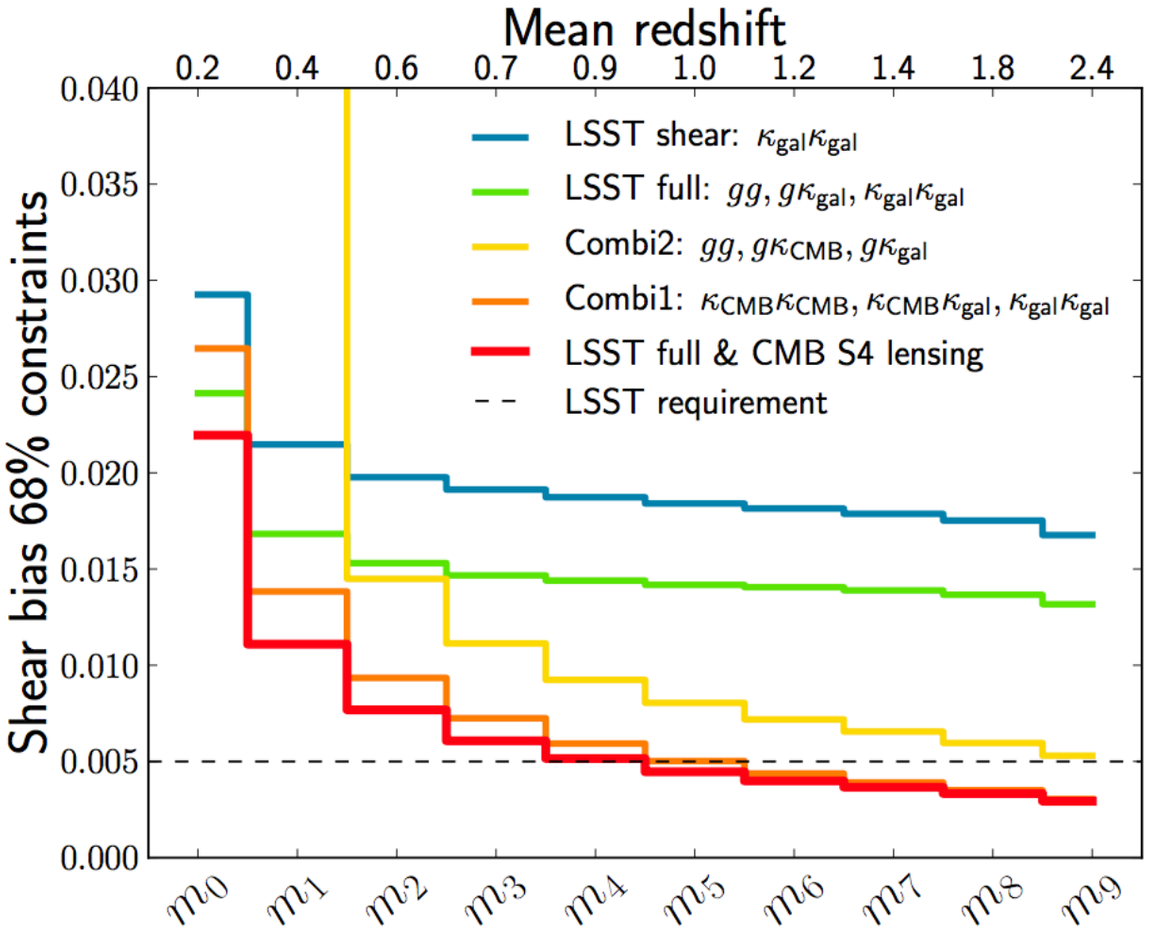

[see talk by Stéphane Ilic]

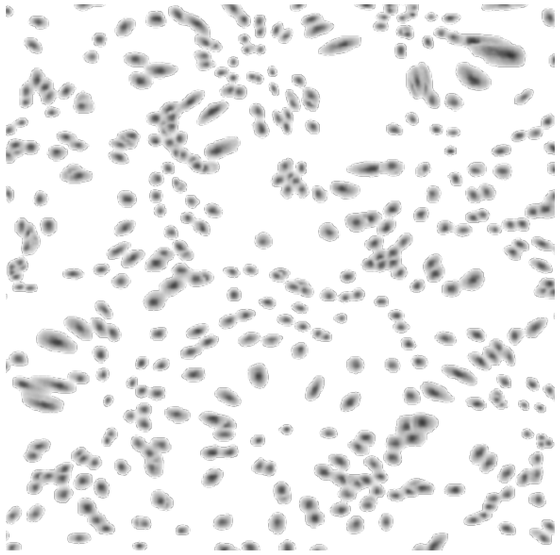

LSST

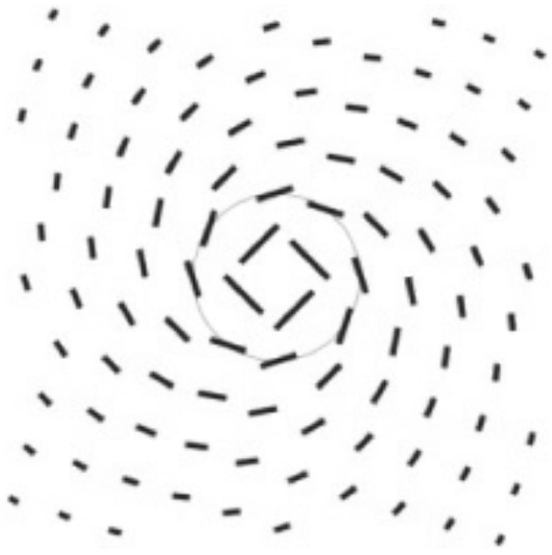

CMB-S4

$$e_g \sim (1+m)\gamma$$

[see talks by Martin Kilbinger and Agnes Ferté]

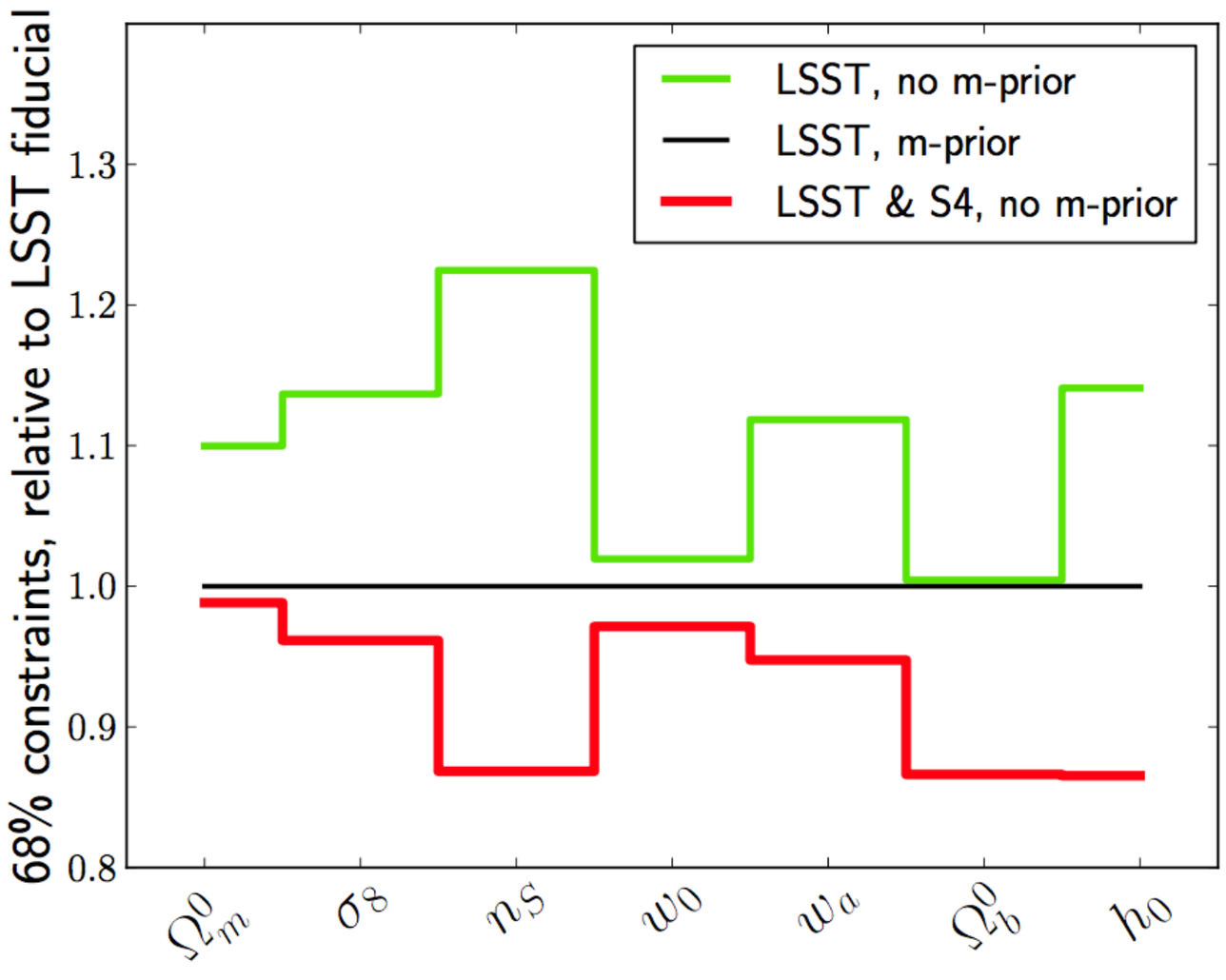

Conclusions

- CMB polarization instrumentation and observations are evolving fast! **Simons Array** (22,000 detectors) is about to start observing, **Simons Observatory** (80,000 detectors) in 2021 and **CMB-S4** (O(500,000) detectors) in ~2025
- CMB is a very sensitive probe to the early and late universe, through the exploitation of 2- and 4-point correlation functions of its polarization maps.

2018 **2021** **2025**

CMB-S4

Conclusions

- CMB polarization instrumentation and observations are evolving fast! **Simons Array** (22,000 detectors) is about to start observing, **Simons Observatory** (80,000 detectors) in 2021 and **CMB-S4** (O(500,000) detectors) in ~2025
- CMB is a very sensitive probe to the early and late universe, through the exploitation of 2- and 4-point correlation functions of its polarization maps.
- there is a great complementarity with e.g. optical and spectroscopic surveys: access to new redshifts (SZ clusters and lensing) and to a good control of systematics (shear biases)

2018 **2021** **2025**

SIMONS ARRAY
POLARBEAR 2017

SIMONS OBSERVATORY

CMB-S4

LSST Large Synoptic Survey Telescope

[see talk by Pierre Antilogus]

DARK ENERGY SPECTROSCOPIC INSTRUMENT

[see talk by Nicolas Busca]

euclid

[see talk by Yannick Mellier]

BACKUP

The unlensed CMB is unobservable but its **statistics** are very well understood — fields are assumed to be **Gaussian** at the primordial level.

The unlensed CMB is unobservable but its **statistics** are very well understood — fields are assumed to be **Gaussian** at the primordial level.

For a flat-sky statistically-isotropic ensemble, harmonics with different $\vec{\ell}$ are uncorrelated i.e.

$$\langle T(\vec{\ell})T(\vec{\ell'})\rangle = \delta(\vec{\ell} - \vec{\ell'})C_\ell^{TT}$$

The unlensed CMB is unobservable but its **statistics** are very well understood — fields are assumed to be **Gaussian** at the primordial level.

For a flat-sky statistically-isotropic ensemble, harmonics with different $\vec{\ell}$ are uncorrelated i.e.

$$\langle T(\vec{\ell})T(\vec{\ell'})\rangle = \delta(\vec{\ell} - \vec{\ell'})C_\ell^{TT}$$

However, the sky we observe is of course not isotropic, and in particular for a given fixed lensing potential, the distribution of the observed temperature will not be isotropic.

➤ we use quadratic off-diagonal terms of the φ-fixed correlation ⟨**T(l)T(l')**⟩ to constrain the lensing potential φ

The unlensed CMB is unobservable but its **statistics** are very well understood — fields are assumed to be **Gaussian** at the primordial level.

For a flat-sky statistically-isotropic ensemble, harmonics with different $\vec{\ell}$ are uncorrelated i.e.

$$\langle T(\vec{\ell})T(\vec{\ell'})\rangle = \delta(\vec{\ell} - \vec{\ell'})C_\ell^{TT}$$

However, the sky we observe is of course not isotropic, and in particular for a given fixed lensing potential, the distribution of the observed temperature will not be isotropic.

➤ we use quadratic off-diagonal terms of the φ-fixed correlation ⟨**T(l)T(l')**⟩ to constrain the lensing potential φ

To estimate the lensing potential on the observed sky, we perform a weighted average of the off-diagonal terms, defining the **quadratic estimator**

$$\phi(\vec{L}) \equiv N(\vec{L}) \int \frac{d^2\vec{l}}{2\pi} T(\vec{l})T^*(\vec{l} - \vec{L})g(\vec{l}, \vec{L})$$

some weighting function

unbias estimator requires that $\langle \phi(\vec{L}) \rangle_{TT} = \phi(\vec{L})$

$$\Big(N(\vec{L})\Big)^{-1} = \int \frac{d^2\vec{l}}{(2\pi)^2} \Big((\vec{L}-\vec{l})\cdot\vec{L}\, C^{TT}_{|\vec{l}-\vec{L}|} + \vec{l}\cdot\vec{L}\, C^{TT}_{l} \Big)\; g(\vec{l},\vec{L})$$

unbias estimator requires that $\langle \phi(\vec{L}) \rangle_{TT} = \phi(\vec{L})$

$$\left(N(\vec{L})\right)^{-1} = \int \frac{d^2\vec{l}}{(2\pi)^2} \left((\vec{L}-\vec{l}) \cdot \vec{L}\, C^{TT}_{|\vec{l}-\vec{L}|} + \vec{l} \cdot \vec{L}\, C^{TT}_{l} \right)\, g(\vec{l},\vec{L})$$

we are then free to choose "g" to maximize the signal-to-noise. One possibility is:

$$g(\vec{l},\vec{L}) \equiv \frac{(\vec{L}-\vec{l}) \cdot \vec{L}\, C^{TT}_{|\vec{l}-\vec{L}|} + \vec{l} \cdot \vec{L}\, C^{TT}_{l}}{2\, C^{tot}_{l}\, C^{tot}_{|\vec{l}-\vec{L}|}}$$

unbias estimator requires that $\langle \phi(\vec{L}) \rangle_{TT} = \phi(\vec{L})$

$$\left(N(\vec{L})\right)^{-1} = \int \frac{d^2\vec{l}}{(2\pi)^2} \left((\vec{L} - \vec{l}) \cdot \vec{L}\, C^{TT}_{|\vec{l}-\vec{L}|} + \vec{l} \cdot \vec{L}\, C^{TT}_{l} \right) g(\vec{l}, \vec{L})$$

we are then free to choose "g" to maximize the signal-to-noise. One possibility is:

$$g(\vec{l}, \vec{L}) \equiv \frac{(\vec{L} - \vec{l}) \cdot \vec{L}\, C^{TT}_{|\vec{l}-\vec{L}|} + \vec{l} \cdot \vec{L}\, C^{TT}_{l}}{2\, C^{tot}_{l}\, C^{tot}_{|\vec{l}-\vec{L}|}}$$

NB: quadratic estimator ≠ optimal estimator

With the above equations, the quadratic estimator finally reads:

$$\phi(\vec{L}) \equiv N(\vec{L})\vec{L} \cdot \int \frac{d^2\vec{l}}{2\pi} \frac{\vec{l} T(\vec{l})}{C^{tot}_{\vec{l}}} \frac{T(\vec{l} - \vec{L})}{C^{tot}_{|\vec{L}-\vec{l}|}}$$